Distribution Category
UC-66

LAWRENCE LIVERMORE LABORATORY
University of California/Livermore, California/94550

UCRL-52094

RESERVOIR ENGINEERING REPORT FOR THE MAGMA-SDG&E GEOTHERMAL EXPERIMENTAL SITE NEAR THE SALTON SEA, CALIFORNIA

R. C. Schroeder
Lawrence Berkeley Laboratory

July 12, 1976

DISCLAIMER

Contents

RESERVOIR ENGINEERING REPORT FOR THE MAGMA-SDG&E GEOTHERMAL EXPERIMENTAL SITE NEAR THE SALTON SEA, CALIFORNIA

Abstract

A description of the Salton Sea geothermal reservoir is given and includes approximate fault locations, geology (lithology), temperatures, and estimates of the extent of the reservoir. The reservoir's temperatures and chemical composition are also reviewed. The flow characteristics are discussed after analyses of drillstem tests and extended well tests. The field production, reserves and depletion are estimated, and the effects of fractures on flow and depletion are discussed.

The reservoir is believed to be separated into an "upper" and "lower" portion by a relatively thick and continuous shale layer. The upper reservoir is highly porous, with high permeability and productivity. The lower reservoir is at least twice as large as the upper but has much lower storativity and permeability in the rock matrix. The lower reservoir may be highly fractured, and its temperatures and dissolved solids are greater than those of the upper reservoir. The proven reserves of heat in the upper reservoir are about 1/4 GW•yr (in the fluid) and 1/3 GW•yr (in the rock). In the lower reservoir the proven reserves of heat are 5-3/4 GW•yr (in the fluid) and 17 GW•yr (in the rock). Unproven reserves greatly exceed these numbers. Injection tests following well completion imply that hydraulic fracturing has taken place in two of the SDG&E wells and at least one other well nearby.

Introduction

A reservoir engineering report usually consists of a collection of all data relating to the reservoir's properties and its production of fluids, followed by an analysis indicating how the reservoir would react to hypothetical production histories. Hydrocarbon reservoirs can be analyzed for primary and some secondary recovery by considering mass flow only. But geothermal reservoirs must be analyzed for both physical and thermal properties of the fluid and

rocks to determine the depletion and flow parameters of the resource during production.

In this report, the analysis will apply to a limited portion of the Salton Sea KGRA.* The Salton Sea KGRA is shown in Fig. 1, along with other KGRA's in the Imperial Valley, and the shaded area inside the Salton Sea KGRA is referred to as the Salton Sea Geothermal Field (SSGF).

The SSGF is an area in which geothermal wells have been drilled and flowed, thus allowing initial indications of the nature of the reservoir and its fluid. Observations

*KGRA is the abbreviation adopted by the U.S. Department of Interior for "known geothermal resource area."

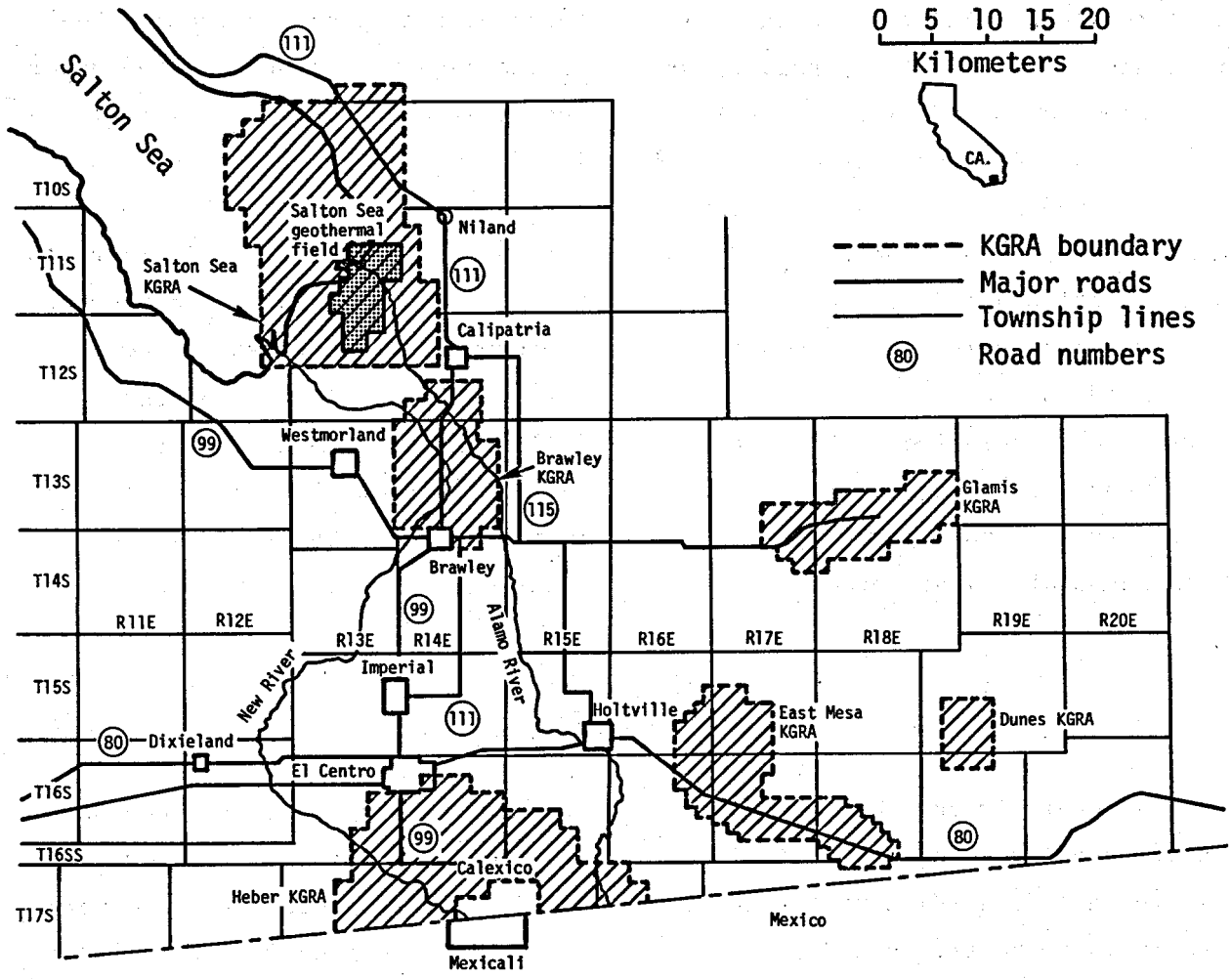

Fig. 1. Map of the Imperial Valley showing the KGRA's and the Salton Sea Geothermal Field (SSGF).

indicate that the SSGF reservoir is liquid-dominated, with current deep temperatures as high as 360 C (680°F). The reservoir fluid is a saline, acidic brine, having up to one-third by weight of dissolved solids.

San Diego Gas and Electric Company (SDG&E) has been involved in geothermal exploration and equipment development in the Imperial Valley since 1971.[1] The Magma lease, on which SDG&E will be operating, is shown by the shaded area in Fig. 2, where the hatched outline denotes the boundary of the SSGF. The current SDG&E plan is to flow two wells during 1976, in order to demonstrate the feasibility of extracting heat from the saline brine. Imperial Magma Company will be selling brine to SDG&E during the planned tests. A total of about 10 MW will be available at two wellheads, and the heat will be dissipated by cooling ponds. Expansion-spray nozzles and natural atmospheric convection will be used for the cooling process.

The equipment to be tested during this well-production period is a system of heat exchangers and steam scrubbers. No useful power will be produced during this initial demonstration period, and some of the spent fluid from the process is to be reinjected into two or more wells. Figure 3 is a closer view of the Magma-SDG&E site, showing the four SDG&E wells and some of the nearby wells outside the area leased by Magma. Magma Power Company's Woolsey No. 1 and Magmamax No. 1 will be the producing wells. The Magmamax No. 2 and No. 3 wells will be used for reinjection, and one or both of the Elmore wells might also be used for reinjection during the test period. Magmamax No. 4 is a shallow well and will be used for observation (monitoring) during production and reinjection. The Sinclair and Elmore wells might also be used for monitoring.

In subsequent sections, we will examine the feasibility of producing 10 MWe or more for an extended time period from the Magma-SDG&E reservoir. In order to do so, a detailed review of the reservoir properties is presented and analyses of some of the wells are used to estimate the reservoir behavior.

As usual, we will find more than one set of units appearing in the figures and calculations. This arises from the desire to use the standardized SI units while most engineering data is presented in either engineering or oil-field units. To make the presentation more coherent, the SI units will usually be used, with engineering or oil-field units

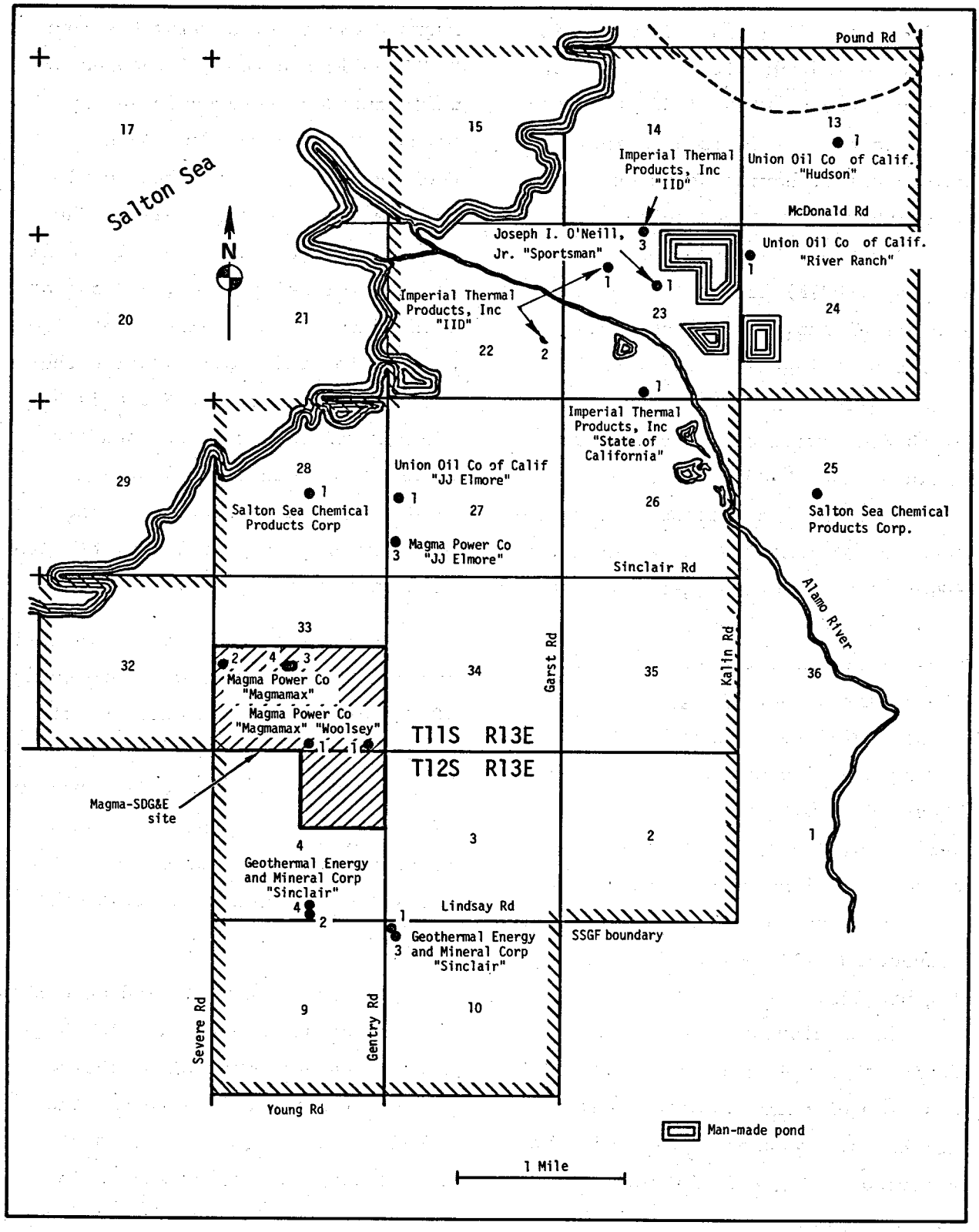

Fig. 2. The location of the Magma-SDG&E lease in the Salton Sea Geothermal Field, Imperial County, California. Base from U.S.G.S. Topographic map. Original scale, 1:24 000. Well information by California Division of Oil and Gas.

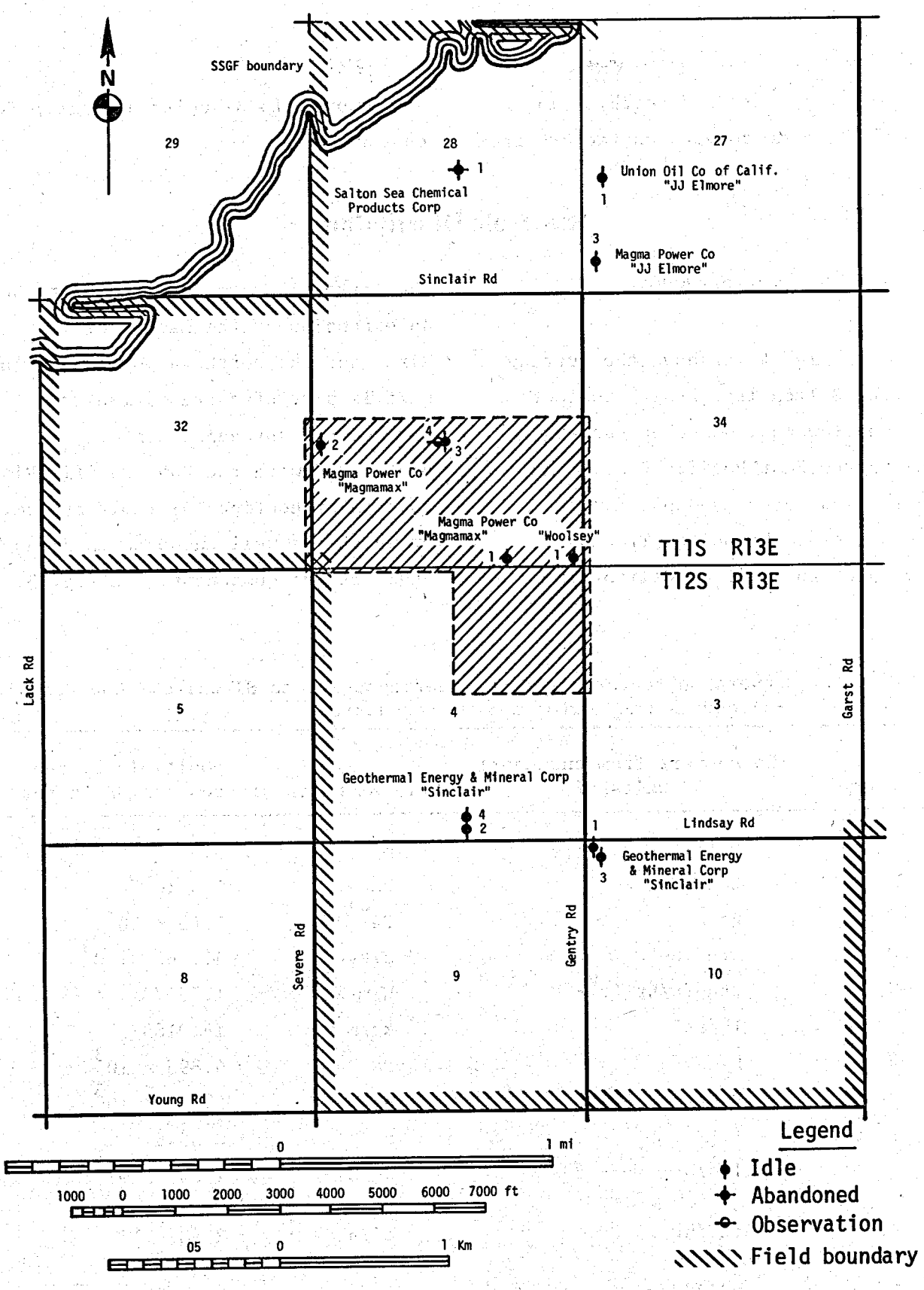

Fig. 3. The Magma-SDG&E site showing wells under study and nearest neighbor wells. Base from U.S.G.S. Topographic map. Original scale, 1:24 000. Well information by California Division of Oil and Gas.

given in parentheses nearby. In Table 1, some conversion factors from engineering to SI units are given for convenience.

Reservoir Description

FAULTS NEAR THE RESERVOIR

In Fig. 4 is shown the setting of the Salton Trough with respect to shallow earthquake epicenters along the East Pacific Rise.[2] An arrow indicates the approximate location of the Salton Trough north of the Gulf of California. The latter feature is believed to be an extension of the East Pacific Rise, and the northern portion of the gulf is part of a transition from the oceanic spreading center associated with the East Pacific Rise to a major continental fault system, of which the well known San Andreas Fault is one component. In Fig. 5,

Table 1. Conversion factors from engineering units to SI units. One Pascal (Pa) equals one Newton per metre squared.

Symbol	To convert from engineering units of	To SI units of	Multiply by the conversion factor
k	millidarcy	m^2	9.87135×10^{-14}
μ	centipoise	Pa·s	1×10^{-3}
β	Psi^{-1}	Pa^{-1}	1.45×10^{-4}
C	Btu/lb-°F	J/kg·K	4.1868×10^{3}
K	Btu-ft/hr-ft^2-°F	W/m·K	1.73073
ρ	lb/ft^3	kg/m^3	16.0185
P	Psi	Pa	6.895×10^{3}
H	Btu/lb	J/kg	2.325×10^{3}
r, D	ft	m	0.3048
q	lbs/hr	kg/s	1.26×10^{-4}
$k/\phi\mu\beta$ or $K/\rho C$	ft^2/hr	m^2/s	2.58×10^{-5}
k/μ	millidarcy/centipoise	$m^2/Pa \cdot s$	9.87135×10^{-11}
ρg	Psi/ft	Pa/m	2.26×10^{4}
kh	millidarcy-ft	m^3	3×10^{-14}

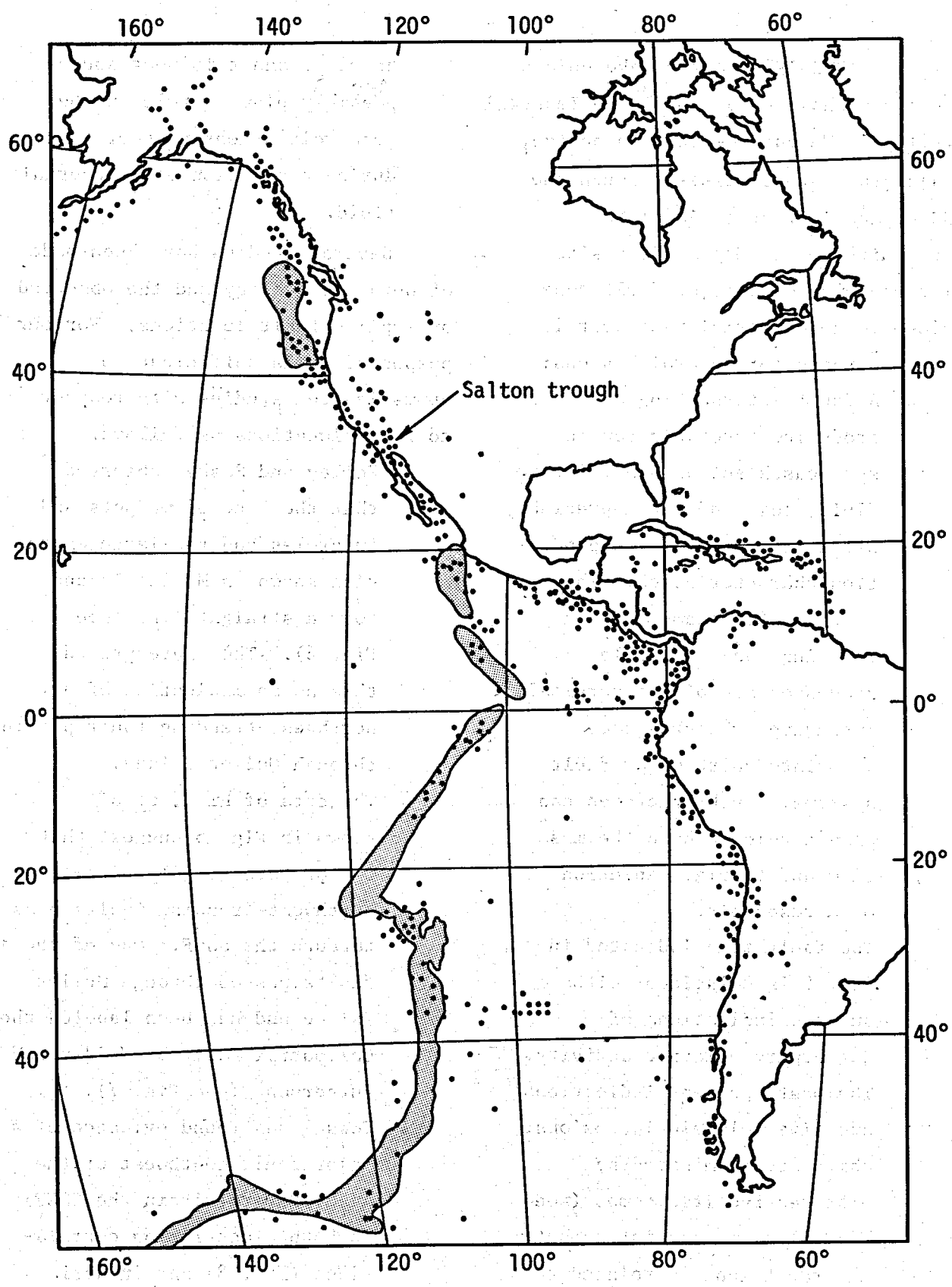

Fig. 4. Relation of Salton trough to the distribution of shallow earthquakes along the East Pacific Rise. From Ref. 2.

recent (1973-1974) earthquake epicenters are shown on a map of the Imperial Valley.[3] We can see that an active, major fault zone passes through the SSGF, and in fact is in close proximity to the Magma-SDG&E site. The presence of a major fault zone close to a geothermal reservoir is of importance for several reasons:

- A fault intersecting a producing reservoir can in some cases act as a barrier to fluid flow, and can appreciably affect the reservoir's production characteristics. This happens, for example, when existing sand and shale sequences are offset vertically.
- Extensive fractures are associated with major fault systems. Such fractures can play a role in both the mass flow and thermal depletion of a reservoir.
- The fault zone indicated in Fig. 5 is coincident with surface indications of Quaternary volcanic activity.[4,5] The most apparent indications are five volcanic intrusions, which are terminated by extruded ryolitic domes (see Fig. 6). One can infer that the fault zone is related to a magmatic heat source, which has produced the geothermal anomaly, and this heat source possibly plays a role in the reservoir's heat regeneration during production of geothermal fluid.

Several studies have been made of both the geology and the observed or implied fault locations. For our purposes, it is sufficient to summarize the studies with respect to fault locations as follows.

- Kelley and Soske[4] observed that the line of mudpots and fumaroles and the large extrusion known as Mullet Island form a straight line (see Fig. 6). They interpreted this as an indication of a northwest-trending fault passing through Mullet Island.
- The data of Hill, et al.,[3] shown in Fig. 5 suggest that two or more roughly parallel northwest-trending faults pass through the SSGF. One of the faults passes through Mullet Island and has been labeled the Calipatria Fault by Meidav and Furgerson[6] (see Fig. 7).
- Towse[7] has found evidence of a major fault southwest of the Alamo River (within the SSGF) in both electric log correlations (Fig. 8) and in aerial reconnaissance photographs. Meidav and Furgerson refer to

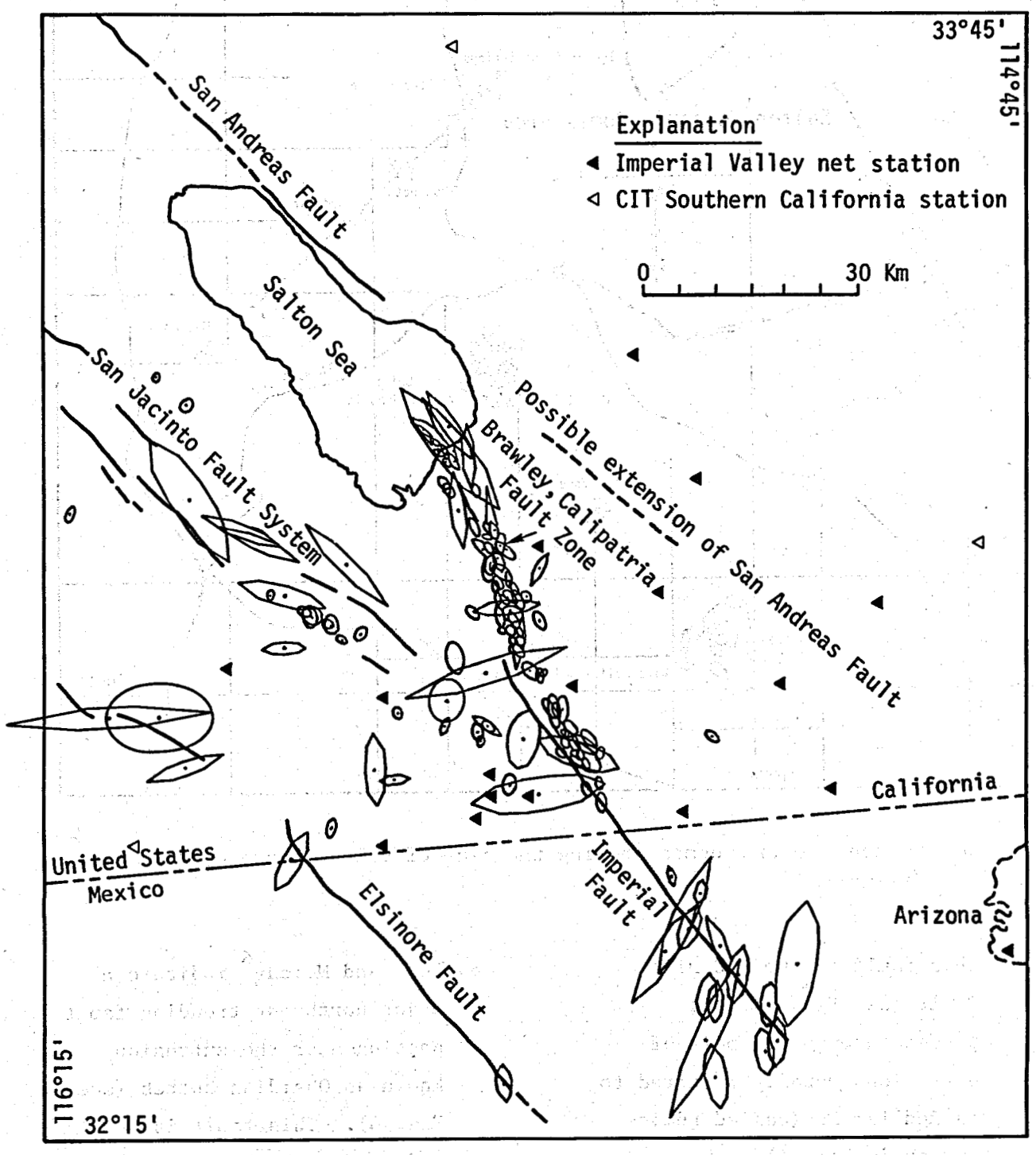

Fig. 5. Map projections of confidence ellipses for earthquake epicenters in the region of the geothermal reservoir under study. From Ref. 3.

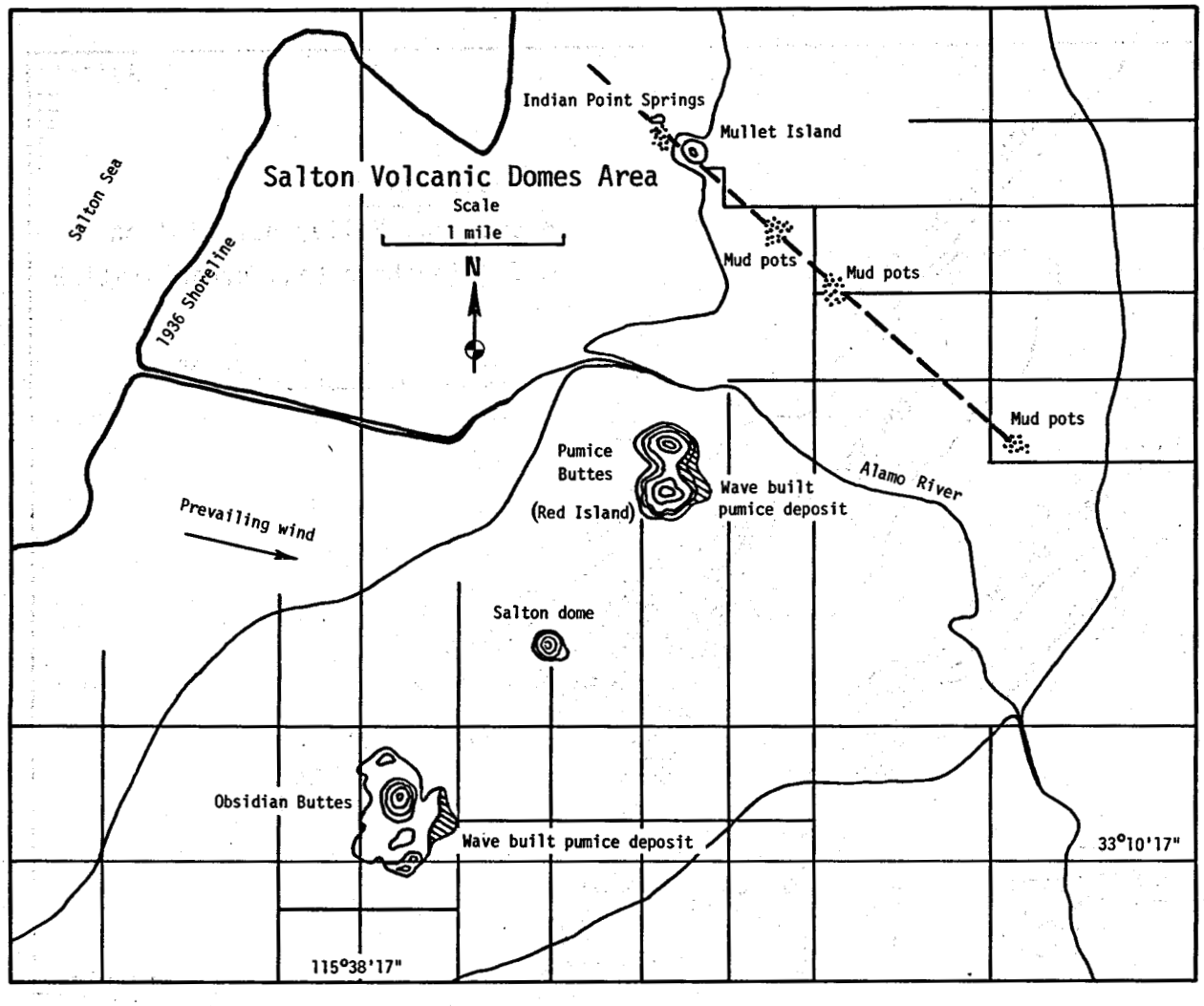

Fig. 6. Salton volcanic domes showing the line of volcanic phenomena. From Ref. 4.

this fault as the Red Hill Fault (see Fig. 7). It passes through the pair of extrusions usually referred to as Red Island (called Pumice Buttes in Ref. 4).

- Biehler and Kasameyer[8] have located the approximate position of the Red Hill Fault near the SSGF's southeast boundary using seismic refraction.
- Lee[9] and Meidav[6] indicate a major northwest-trending fault passing near the extrusion known as Obsidian Buttes (see Fig. 6). This fault is referred to by both as the Brawley Fault. The picture that has unfolded from these studies is shown in Fig. 9. The faults passing through Mullet Island and Red Island

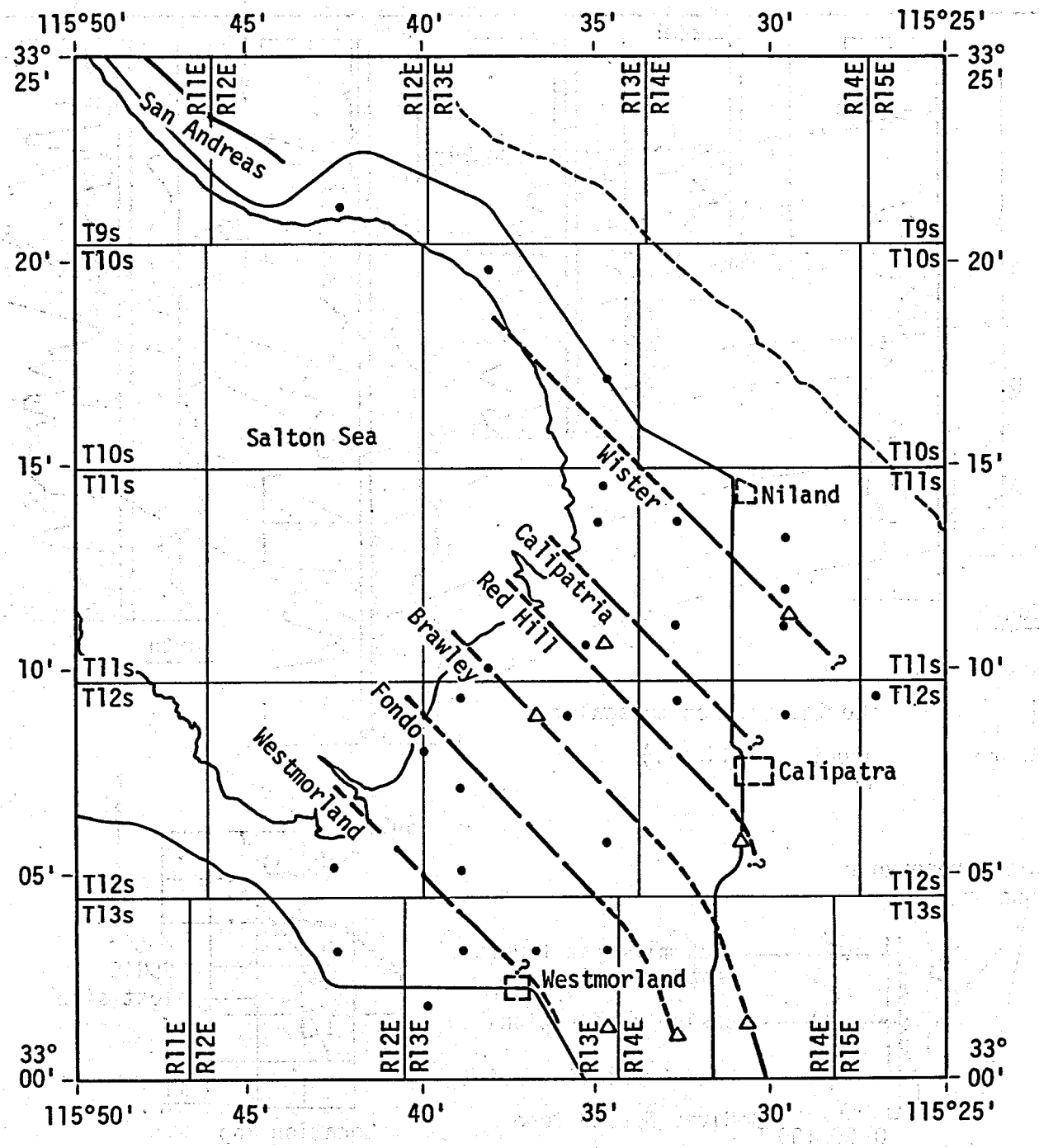

Fig. 7. Map of possible faults and discontinuities in the Salton Sea area. From Ref. 6.

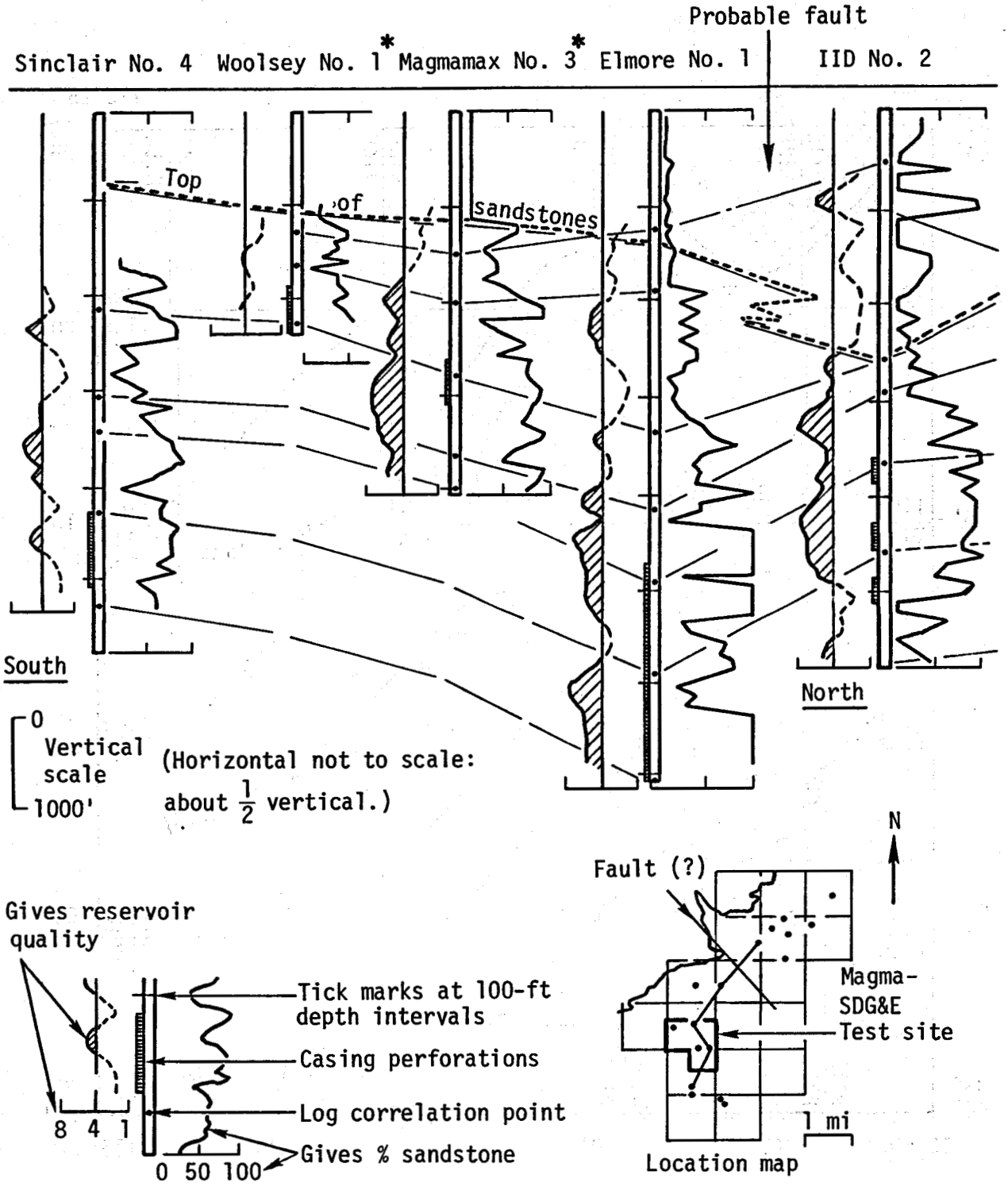

*Woolsey 1 and Magmamax 3 are test site wells on the section.

Fig. 8. North-south cross sections of well logs and their lithofacies interpretation. "Reservoir quality" is a lithofacies interpretation of permeability and continuity: 8 = 'good'; 4 = 'fair'; 1 = 'poor.' From Ref. 7.

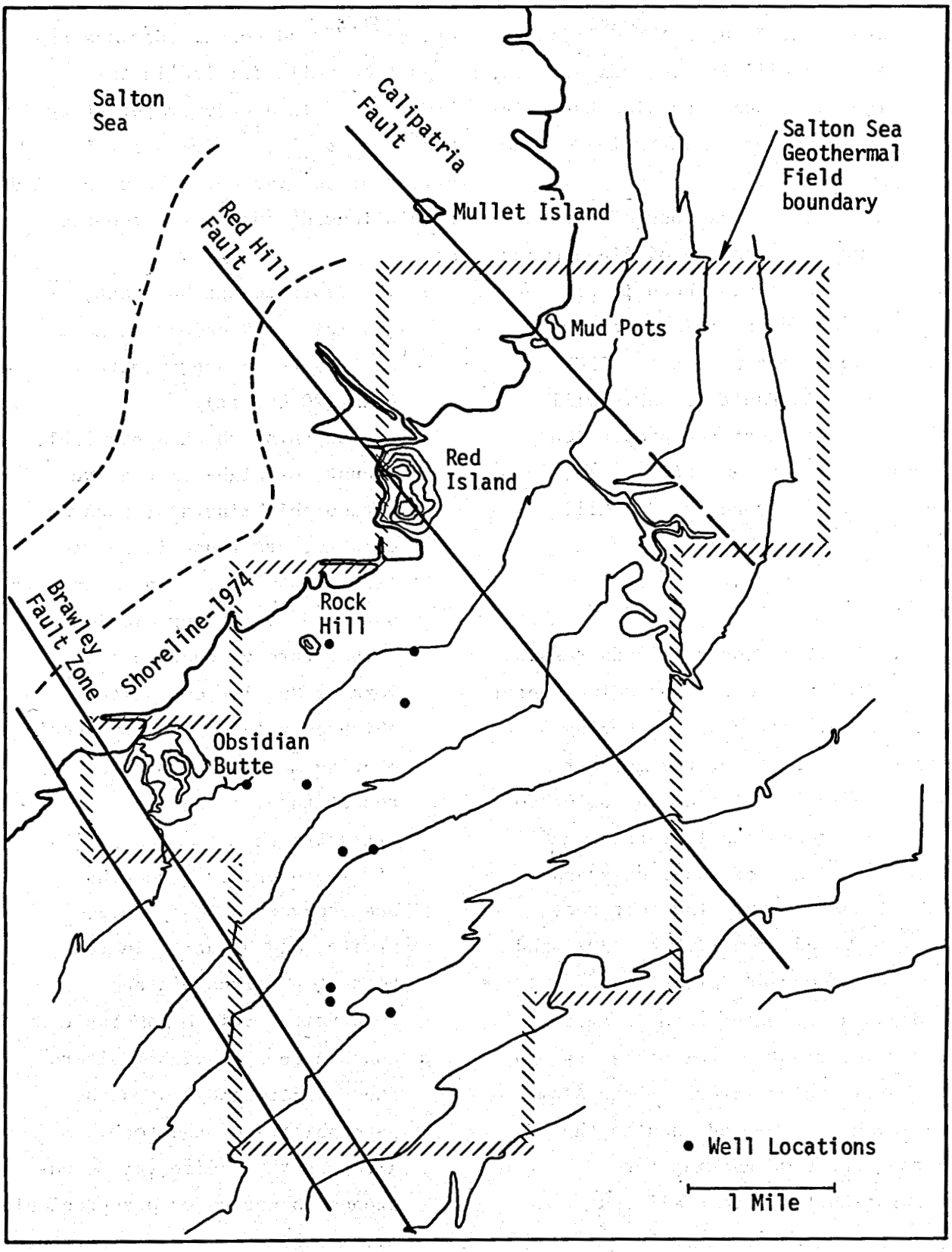

Fig. 9. Topography of the Salton Sea Geothermal Field showing the extruded domes and the approximate fault lines.

are identified as the Calipatria and Red Hill Faults, respectively. The fault near Obsidian Butte is indicated as an extension of the Brawley Fault.

The precise locations of the faults and their angles of dip are not known, but the lines shown in Fig. 9 are believed to approximate their surface locations within the SSGF. The Calipatria Fault probably will not directly affect the production behavior at the Magma-SDG&E site, since it lies beyond the Red Hill Fault.

GEOLOGY

The Salton Trough is a depression that is related to the spreading center of the East Pacific Rise. During recent geologic time, the meanders and periodic flooding of the Colorado River have deposited lacustrine and deltaic deposits of sand, silt and clay in the trough. The most recent flood occurred from 1905 to 1907, and formed the current Salton Sea.[10] Colorado River water used in agricultural irrigation now makes its way to the two major rivers -- the Alamo and New Rivers -- and then to the Salton Sea, compensating for evaporation. The rainfall and associated runoff is small.

The area's geology has been studied by observations of outcrops,[11,12] and cores, cuttings and logs from wells drilled in the SSGF.[13,14] In a groundwater study, Dutcher, et al.,[15] give a large number of references. The simplified conclusions of these many reports are:

- The depth to the basement, granitic rock under the Magma-SDG&E site is approximately 6 km (20 000 ft).[15]
- The depth at which appreciable amounts of high-temperature metamorphic minerals, such as epidote, are found is about 1100 m (3500 ft). This depth is obtained from a correlation of temperature vs depth and the work of Muffler and White,[16] which correlates the SSGF sedimentary metamorphism with temperature. Helgeson[17] estimates that as much as 25% of the reservoir's rock has been converted to epidote, pyrite, and hematite in the hottest portions of the reservoir. This metamorphic conversion appreciably alters the porosity and lowers the permeability of the rock. Although the sedimentary sandstones do not undergo appreciable metamorphism even at temperatures as high as 400 C, the shales, silts, etc., undergo appreciable

metamorphism above 300 C. Hydrothermal transport of these metamorphosed minerals in the permeable sandstone may be accompanied by precipitation, which would decrease the sandstone's porosity and permeability.

- The reservoir rock is overlain with a shale bed about 350 m (1150 ft) thick, which partially insulates the reservoir (thermally) from the atmosphere.[14] This reservoir cap rock also has very low permeability.[15]
- The main sequence reservoir rock is bedded sandstone with shale lenses and layers. The Magma-SDG&E reservoir might be separated into two parts by a shale layer approximately 12 m (40 ft) thick. This shale layer has been correlated on electric logs taken from all four Magma-SDG&E wells.[14] It is not known whether fractures exist in the shale to provide vertical permeability, or whether the reservoir is actually separated into two portions. Towse and Palmer[14] refer to the main sequence rock as "upper" and "lower" reservoirs. The respective thicknesses are about 450 m (1500 ft) and more than 1000 m (3300 ft). The approximate depths of the separating shale layer near the Magma-SDG&E site are shown in Fig. 10.
- Within the main sequence reservoir rock (excluding several identifiable shale layers), the percentage of sandstone is often greater than 50%, averaged over about 30 m (100 ft).[14,18]
- Estimates of average sandstone porosity in the reservoir range from about 15 to 30% (excluding shale).[15,19]
- The main sequence reservoir rock appears to be highly fractured in some areas.[17] Rock well below the metamorphic transition depth of about 1100 m obtained from the State No. 1 well (located about 4 km NE of the Magma-SDG&E site) also showed a large number of cracks.

TEMPERATURES WITHIN THE RESERVOIR

Measurements have been made throughout the SSGF, providing profiles of temperature vs depth. In Fig. 11, the temperature-depth profiles for the Magma-SDG&E wells and some of the nearest neighbor wells are shown. Helgeson[17] discusses the implications of the temperature profiles and concludes that, although temperature gradient

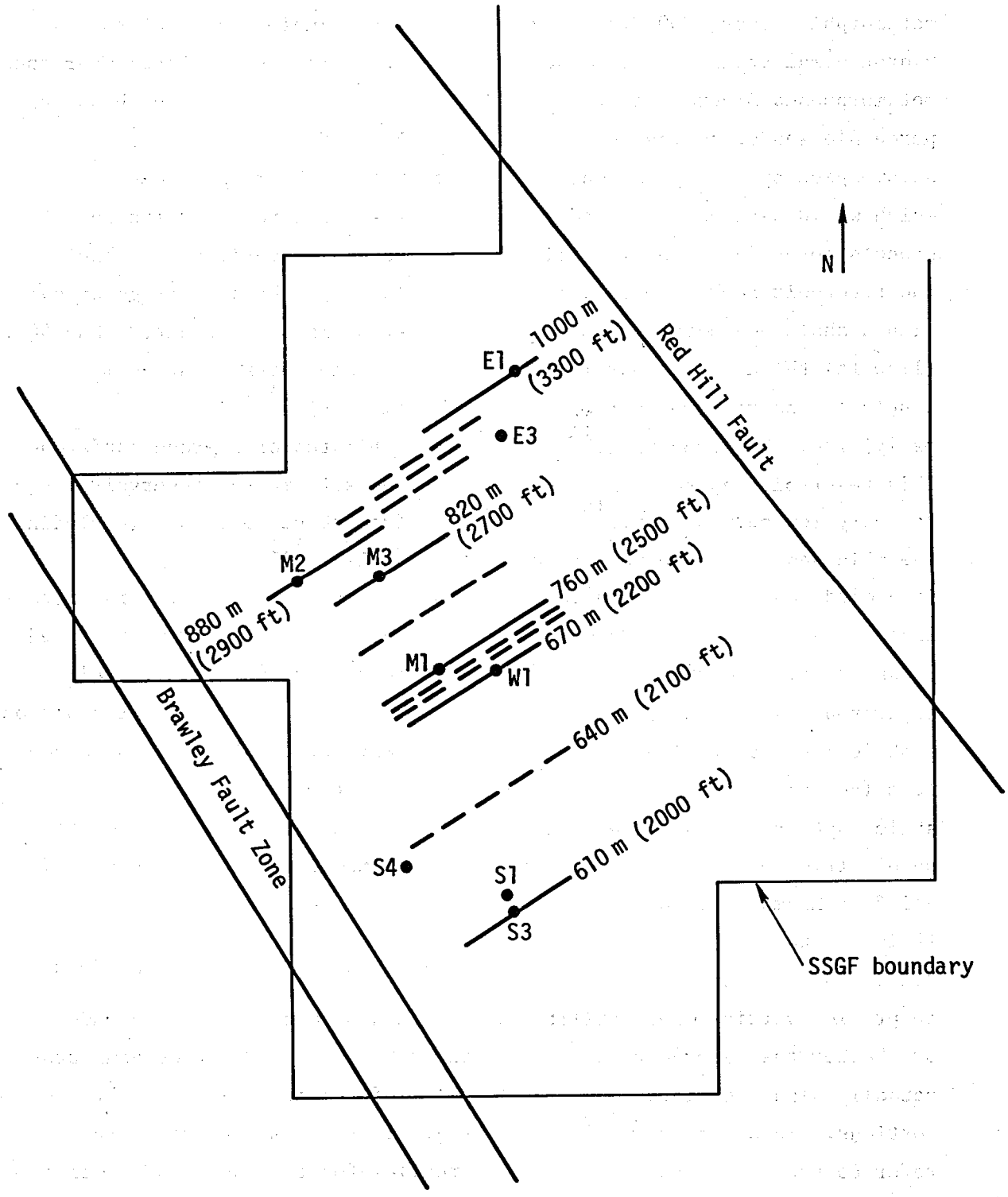

Fig. 10. Approximate depth to the major shale break separating the upper and lower reservoirs of Towse. Lines show assumed contours of depth. Approximate locations of major faults are labeled. The wells are identified by a letter and a number: Magmamax No. 1 = M1, Elmore No. 1 = E1, Sinclair No. 1 = S1, and Woolsey No. 1 = W1.

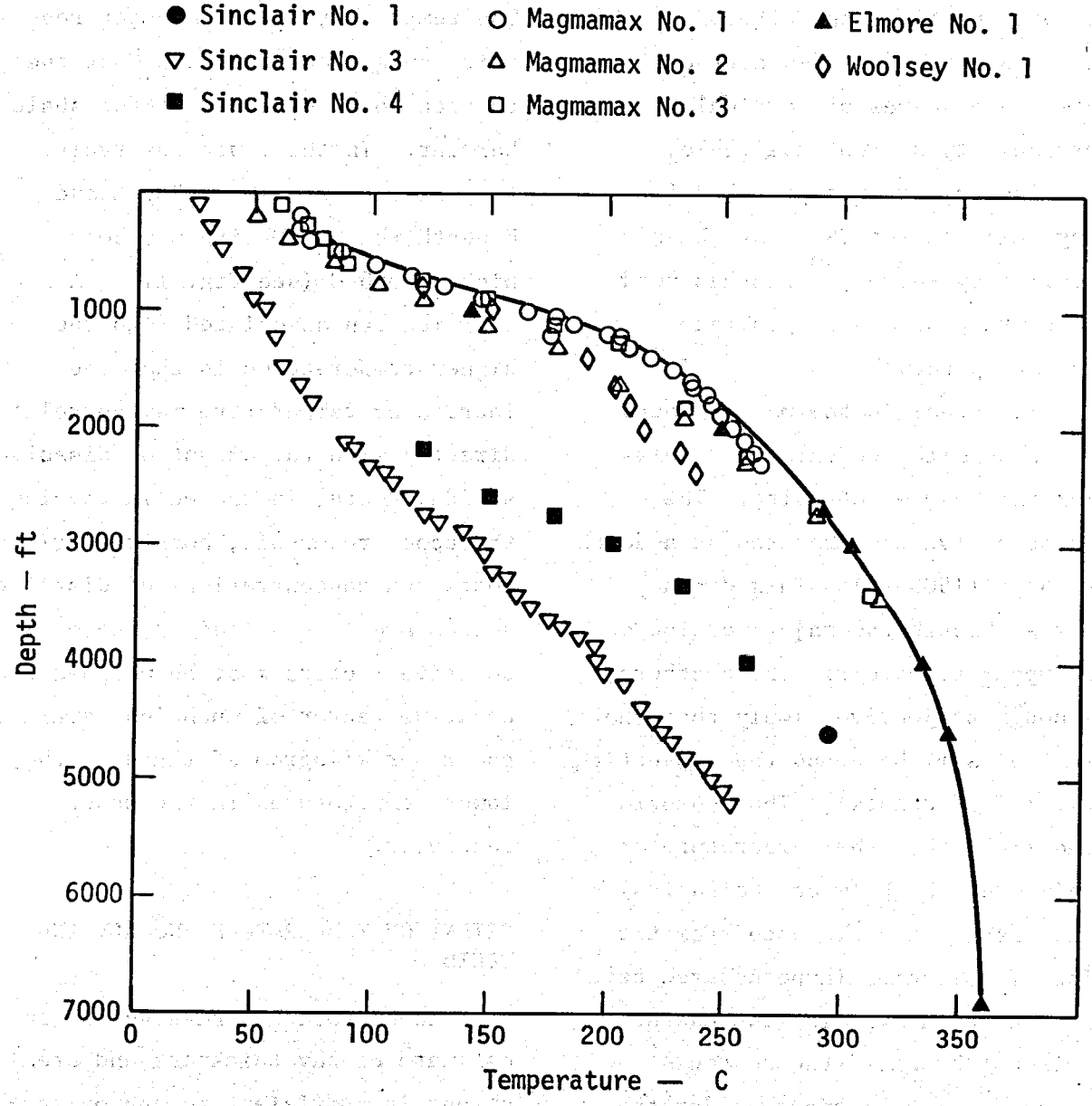

Fig. 11. Temperature-depth profiles for the Magma SDG&E wells and some nearest neighbor wells.

values of about 0.4 K/m (0.55°F/ft) give a reasonable heat flow at the surface equal to 0.75 W/m^2 (about 17 HFU*) (when the mechanism is assumed to be heat conduction in the caprock), the much smaller temperature gradients below the caprock imply that the heat-flow mechanism is probably convection. The only problem with using the concept of large-scale convective heat transfer to model the reservoir is that, at

*1 HFU = 1 $\mu cal/cm^2 \cdot s$

the present time, the effects of the shale layers and lenses are not known, and values of vertical permeability are not available.

The temperature profiles for many wells in the SSGF have been compiled by Palmer,[20] who has used the depth profiles to generate areal temperature contours. In Fig. 12, areal isothermal contours are shown with the existing faults near the Magma-SDG&E site. The contours give temperatures at a depth of 457 m (1500 ft). This depth passes through the major portion of the upper reservoir. The contours, although subjective, imply that the two faults might bound the convecting cell (if it exists). The contours also imply that the temperature at a given depth (between the faults) decreases as the distance from the line of volcanics (hypothesized heat axis shown in Fig. 12) increases. It is not known if the contours extend an equal distance under the Salton Sea from the volcanics.

From these observations, it appears that the Magma-SDG&E and the Elmore sites are well situated with respect to the depth to the upper reservoir, hence require less drilling. However, the upper reservoir between the depths of 335 m (1100 ft) and 915 m (3000 ft) is cooler than the lower reservoir. The temperatures in the upper reservoir range from about 200 C at the caprock to about 300 C at the shale barrier. In the lower reservoir, temperatures are above 280 C and beneath the SDG&E site may be as high as 360 C (see Fig. 11). A complication associated with the higher temperatures is that the increasing temperature may correlate directly with the amount of dissolved solids. Hence, in the wells tapping the upper reservoir, both the drilling costs and concentrations of dissolved solids are less. Against these positive factors must be weighed the negative factor of much less available power per kilogram of fluid at the lower temperatures in the upper reservoir.

EXTENT OF TEMPERATURE ANOMALY AND FLUID

In hydrocarbon reservoirs, an estimate of pay thickness and areal extent is sufficient to approximate the size of the resource. For geothermal reservoirs more factors must be evaluated. Not only is the extent of the reservoir's fluid a required value, but the extent of the heat is as well. The total areal extent of the fluid at the Magma-SDG&E site is not known, but it appears from the data at neighboring wells that the reservoir rock is

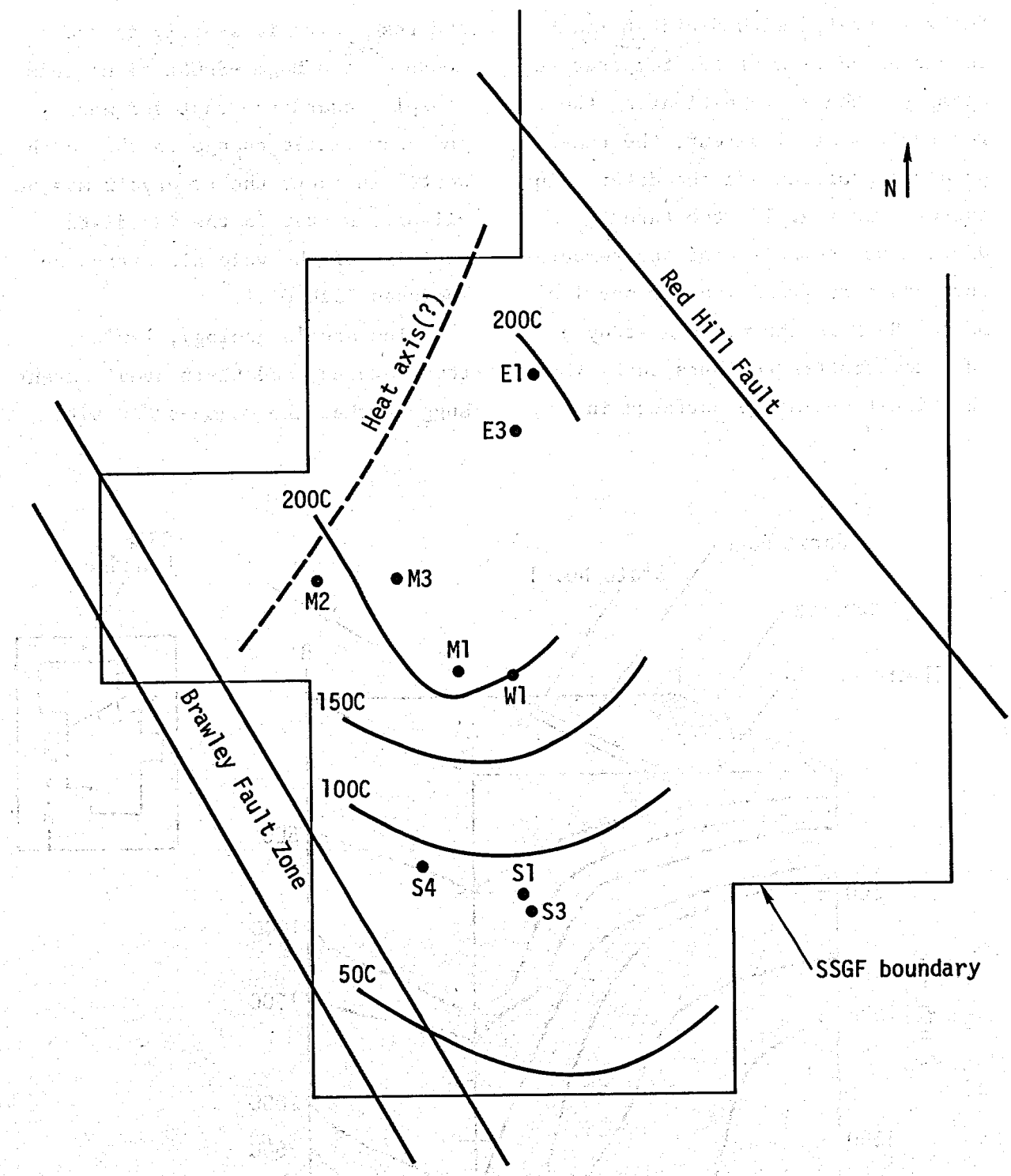

Fig. 12. Temperature contours at 457 m (1500 ft) below ground level with approximate fault locations shown. The dashed line is the approximate axis of the volcanic intrusions. At greater depths, the 200 C contour encompasses much more area. The wells are identified by a letter and a number: Magmamax No. 1 = M1, Elmore No. 1 = E1, Sinclair No. 1 = S1, and Woolsey No. 1 = W1.

fully saturated with fluid at least to the boundaries of the temperature anomaly. Hence, in estimating the reservoir's areal extent, the temperature profiles are the determining factor. In Fig. 13, the three-dimensional composite of the temperature contours from a narrow section of the SSGF is shown.[21] A study of such temperature contours shows that the high-temperature surfaces in the reservoir dip steeply to the south of the Magma-SDG&E site, less steeply toward the east and north, and show little change to the northwest. In fact, the reservoir may be slightly hotter in the immediate vicinity of the volcanic extrusion known as Rock Hill.

The area's geology, faults, temperatures, and their areal extent suggest that the Magma-SDG&E site

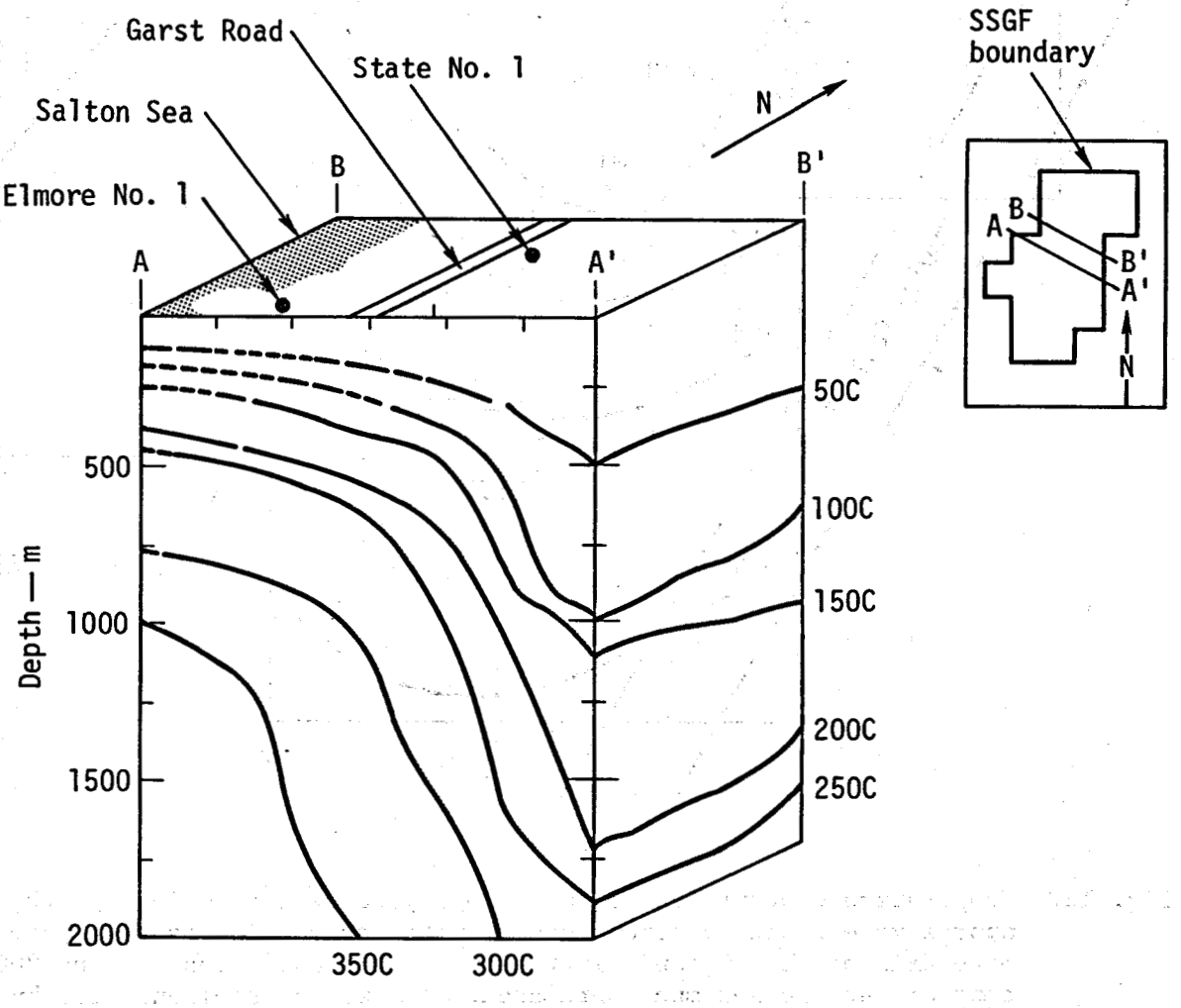

Fig. 13. Block diagram of isothermal surfaces, Salton Sea Geothermal Field after Palmer[21]. Vertical is exaggerated 4x.

is on the southeastern flank of both the upper reservoir and the major, lower (or deep) reservoir. A crude estimate of the volume of the reservoir in the vicinity of the Magma-SDG&E site is obtained as follows.

Upper reservoir: The upper reservoir between Brawley and Red Hill Faults has a caprock of approximately constant thickness, but Fig. 10 shows that the shale layer separating the upper and lower reservoirs dips to the northwest. The areal extent within the average 200-C contour is estimated to be at least 10 km^2 (4 mi^2). This is an area that does not include any of the region under the Salton Sea and is within the bounds of the Brawley and Red Hill Faults. The average upper reservoir thickness in this region is about 450 m (about 1500 ft). These very rough figures give an approximate upper reservoir volume of 4.5 km^3 between the two faults.

Lower reservoir: The average depth of the bottom of the shale layer defining the top of the lower reservoir is about 760 m (2500 ft). Choosing a total depth for the lower reservoir is more difficult, but the deepest well in the vicinity of the Magma-SDG&E site is the Elmore No. 1 well, which was drilled to about 2100 m (7000 ft), at which point igneous rock began appearing in the sediments. The lower reservoir thus appears to have at least 1000-m thickness down to volcanics that may or may not be impermeable. The areal extent of the lower reservoir is unknown, but we can conservatively take the same area used for the upper reservoir. This gives a total extent for the lower reservoir of about 10 km^3. The total volume of fluid and sand, shale and other rock types is then at least 14 km^3. Note that this is an estimate of the reservoir volume containing both fluid and rock. It is important to note that the system of wells at the Magma-SDG&E site is not near the center of the large block system formed by the Brawley and Red Hill Faults but is closer to the Brawley Fault Zone. Thus, the Brawley Fault might affect the well system during production.

The size and depth of the heat source probably determines the extent of the temperature anomaly. In Fig. 14, the magnetic anomaly map of Kelley and Soske[4] is shown, and in Fig. 15 the more recent map of Robinson et al.[5] is given. In

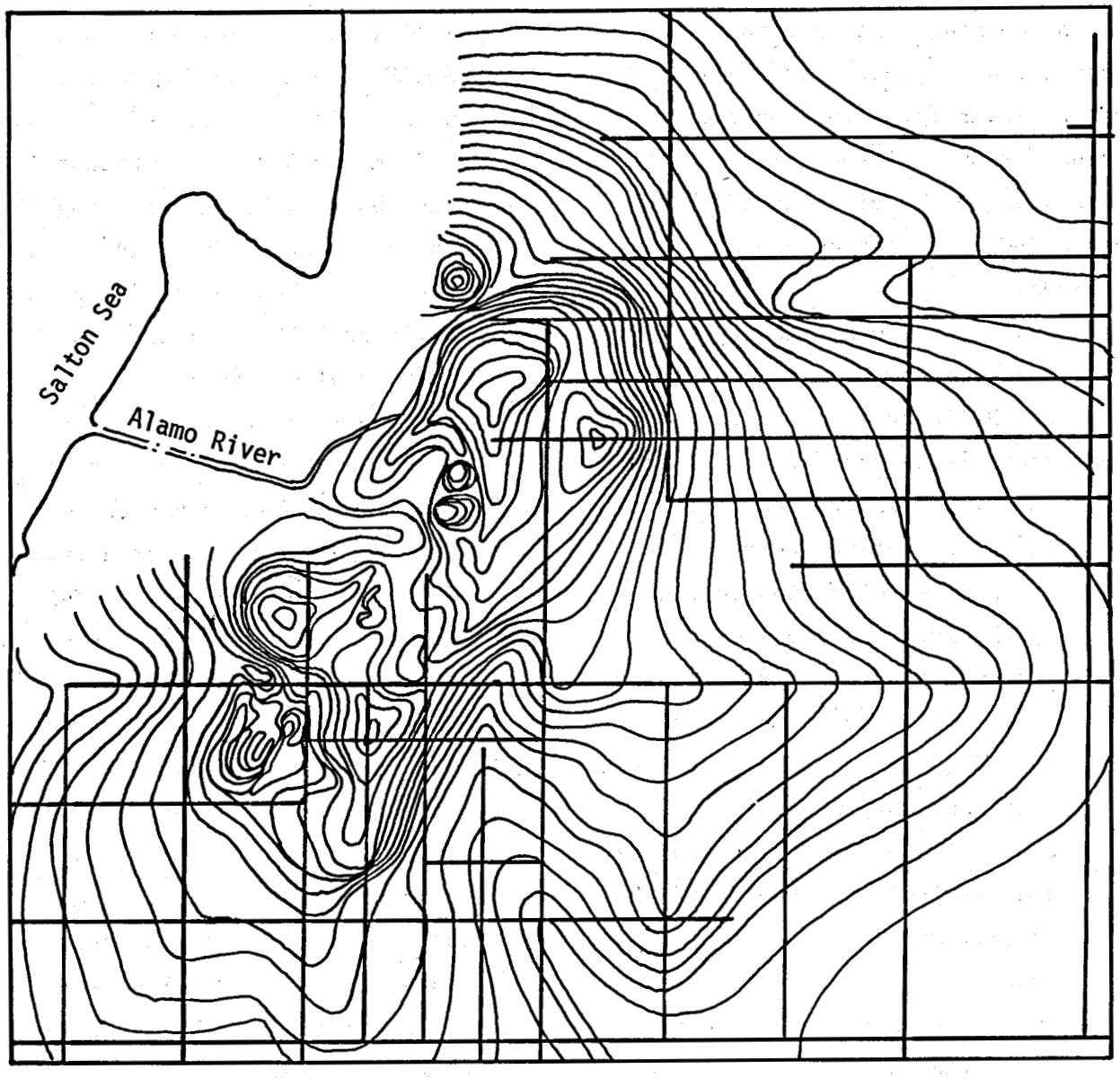

Fig. 14. Isonomalic vertical intensity map of Salton volcanic domes area. From Ref. 4.

Fig. 16 the Bouguer anomaly map[22] is shown. All of these geophysical studies have been interpreted to imply a deep, extensive, igneous body which is undoubtedly related to the extent of the temperature anomaly. Kelley and Soske[4] picture the volcanic intrusions in the area as very localized, with a mushroom-shaped extrusion at the surface. Biehler points out that the gravity anomaly is positive over the entire Imperial Valley--a surprising observation, given that the relatively low-density sediments are up to 6 km deep in the Salton Trough. Either a thin crust

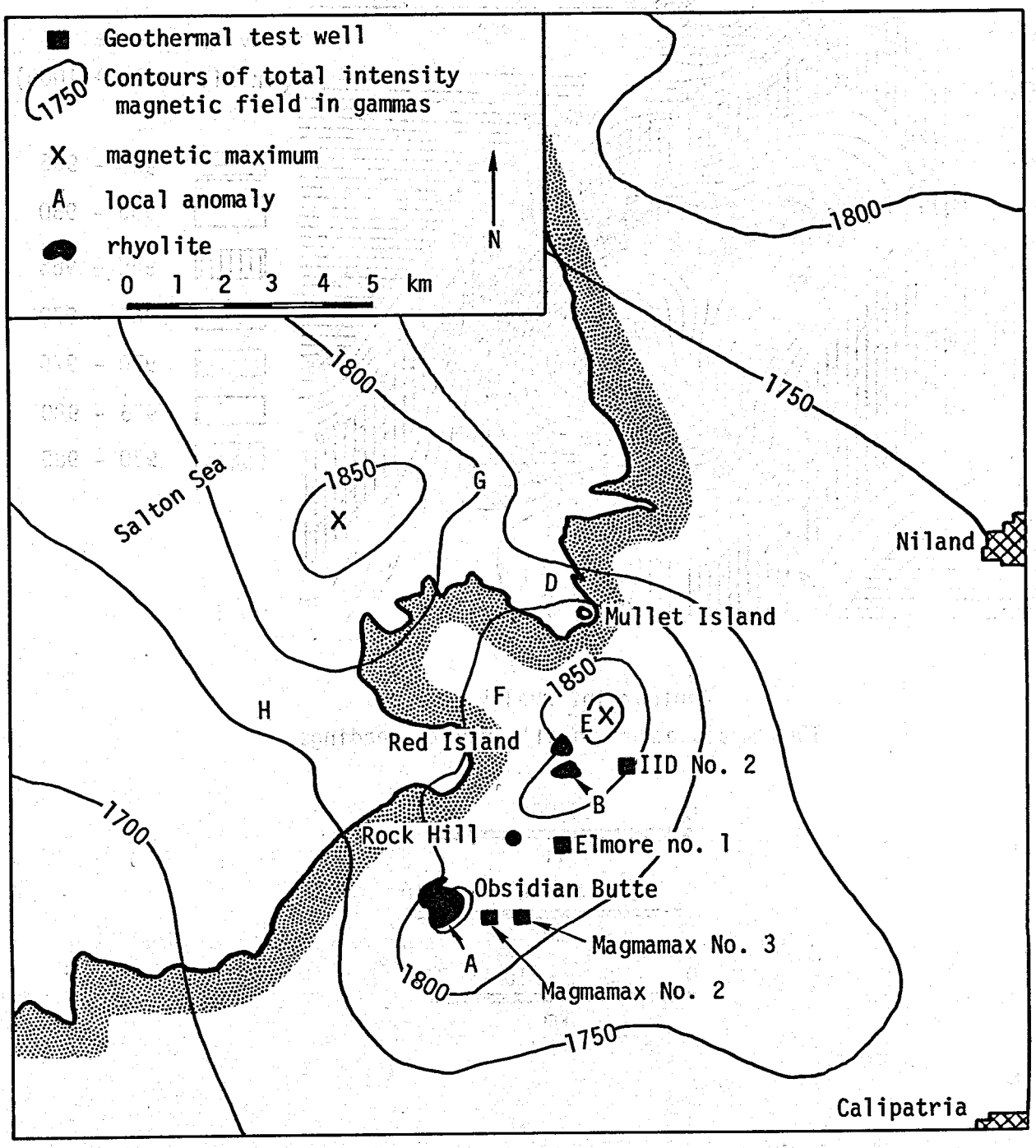

Fig. 15. Map showing Salton Buttes, selected geothermal wells, magnetic anomalies, and magnetic contours. From Ref. 5.

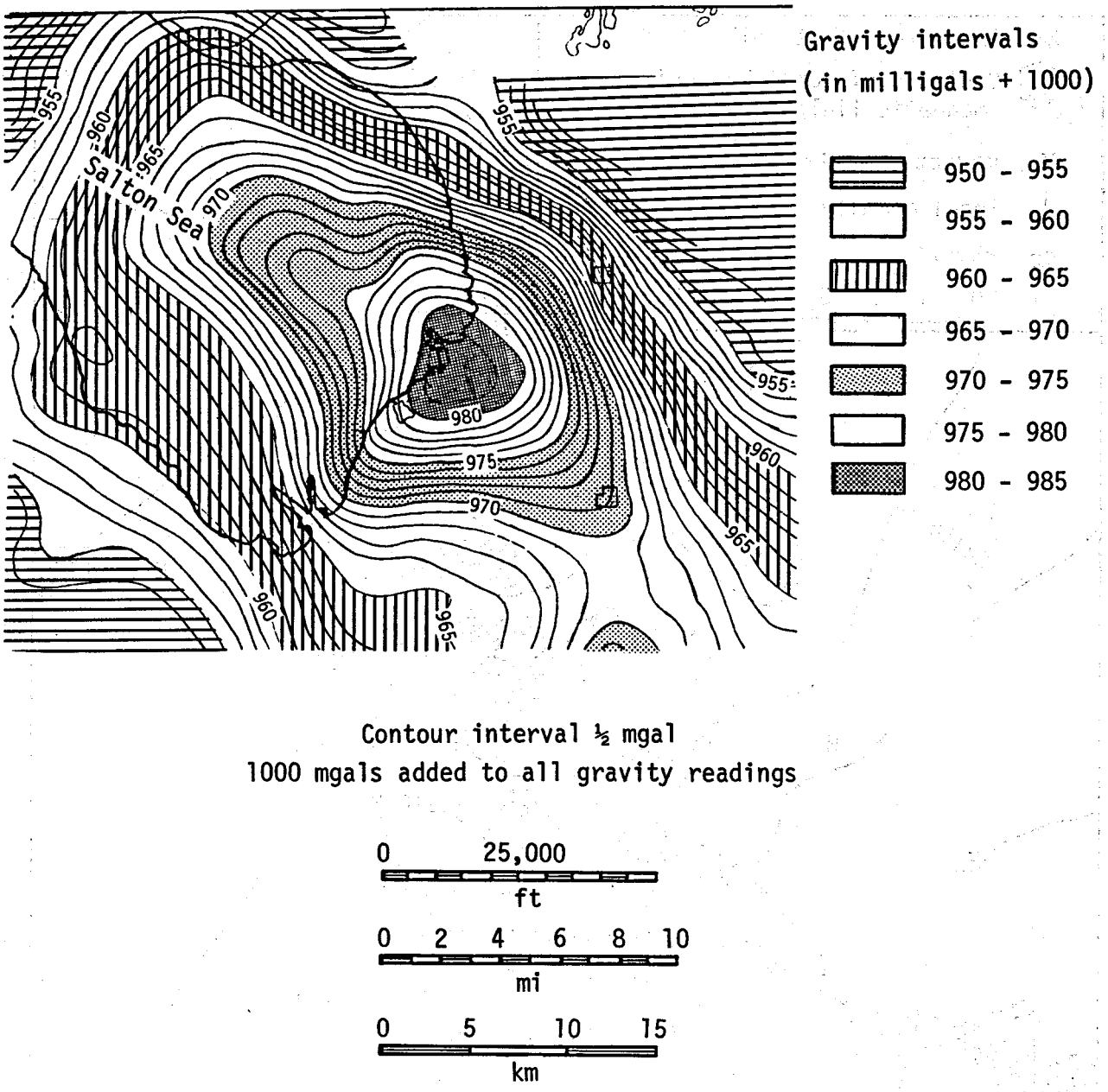

Fig. 16. Complete Bouguer Anomaly map of the Imperial Valley. Contour interval is 1 milligal, Bouguer density 2.67 gm/cc. 1000 milligals added to all contours. From Ref. 22.

or a deep, igneous, intrusive body of higher-density rock can be hypothesized to explain this observation. Note that the Bouguer values are negative in Fig. 16, relative to the basement rock in the mountains flanking the Salton Trough, but the anomaly is peaked positively over the trough and is less negative there than would be expected, given the depths of the sediments. Both the magnetic and gravity anomalies are roughly centered on a portion of the Red Hill Fault, or very close to it.

THERMAL AND CHEMICAL PROPERTIES OF THE FLUID

The thermal and chemical properties of the reservoir's fluid and rock are not well known. An indication of this is seen in Table 2 below, where data for dissolved solids from two of the Magma-SDG&E wells and two nearby wells are given.[20,23] The reasons for the large discrepancies among these data include failure to account for steam loss and incomplete elemental

Table 2. Reported[20,23] thermal and chemical properties of brine from wells in and near the Magma-SDG&E site.

Well	pH	Total of analyzed constituents	Total wt fraction of dissolved solids reported	Bottomhole temperature, C	Well depth, m (ft)
Pioneer Denver Co.	6.5	0.110	0.110	>70	321 (1054)
Magmamax No. 1	6.65	0.284	0.284	265	701 (2300)
		0.218	0.218		
Woolsey No. 1	6.2	0.121	0.132	238	731 (2400)
	6.45	0.088	0.099		
	6.25	0.153	0.151		
Sinclair No. 3	5.3	0.155	0.184	252	2110 (6992)
	4.3	0.233	0.276		
Sinclair No. 4	5.0	0.356	0.388	260	1616 (5300)
	5.3	0.259	0.267		

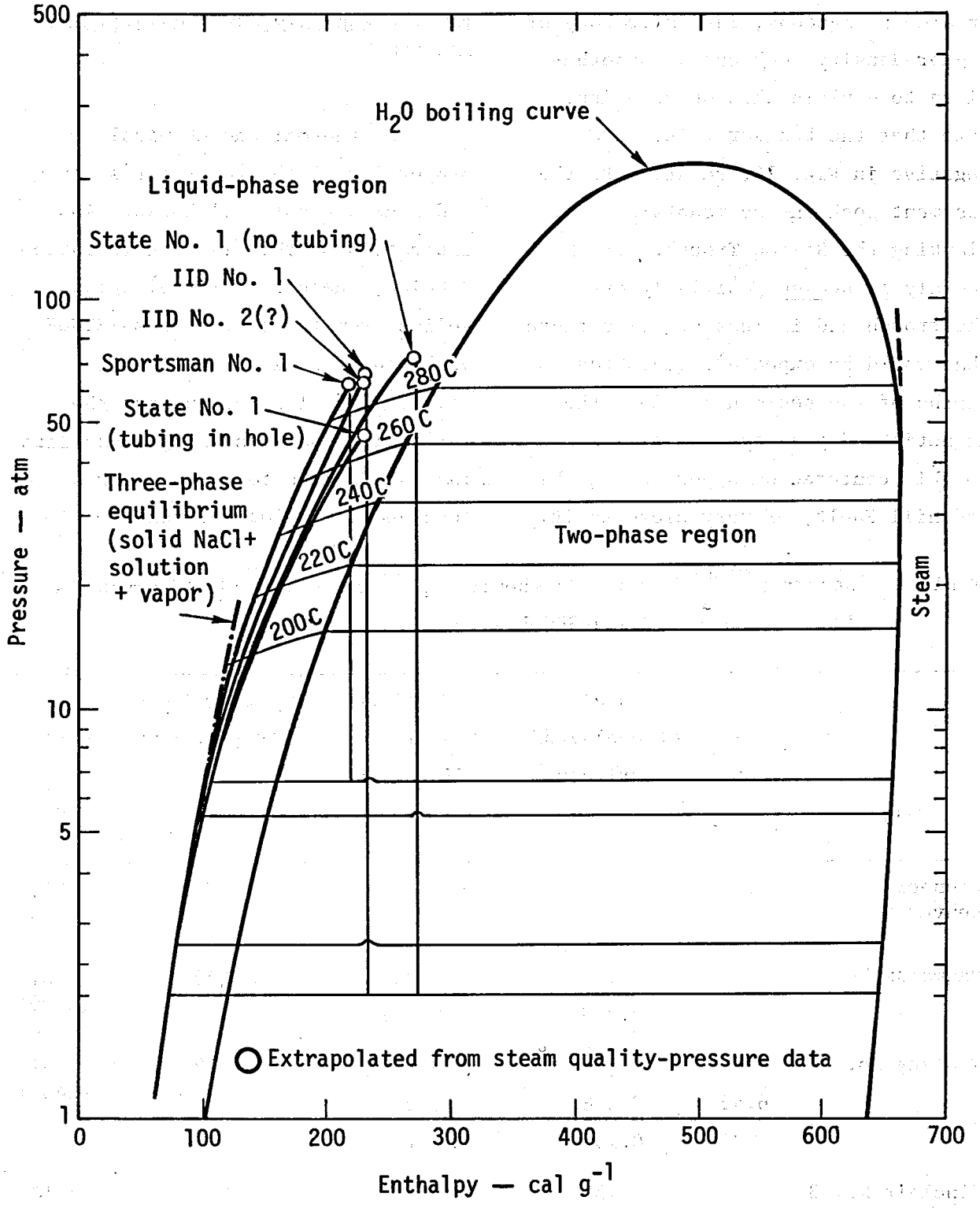

Fig. 17. Abridged enthalpy-pressure diagram for H_2O and the geothermal fluid produced by the wells. The curves shown for the geothermal system were computed. From Ref. 17.

analysis. In addition, the experimental conditions corresponding to the reported values are not made clear. Finally, the analyses were made from brine at the wellhead, where the conditions differ significantly from those in the reservoir. One of the most important considerations, particularly with regard to reinjection, is the presence of silica in the brine and its behavior after reinjection (see, for example, Ref. 24).

In order to estimate the amount of energy that can be extracted from the brine, we must know the brine's equation of state and the values and variation of its temperature-dependent parameters, such as specific heat. Since this estimate involves fluid flow and heat flow, we also need the temperature dependence of such physical and thermal properties as viscosity, compressibility, and thermal conductivity. Figure 17 is the enthalpy diagram from Helgeson,[17] and the temperature dependence of the viscosity is shown in Fig. 18.[25,26] In Figs. 19 and 20,[25,27] the compressibility of water and some typical reservoir rocks, respectively, are given. In Fig. 21, the temperature dependence of the specific heat of water is shown.[28] In subsequent Figs. 22-26, the thermal properties of some typical rocks are given.[29,30]

DESCRIPTIVE SUMMARY

The Magma-SDG&E test site is located between two active faults, which are part of the major tectonic zone responsible for the existence of the geothermal anomaly (SSGF). The reservoir is probably separated into two distinct layers-- the upper and the lower reservoirs. The upper reservoir is capped by a shale layer, which thermally insulates it from the surface. The shale bed separating the upper and lower reservoirs dips toward the line of volcanic intrusions, which may have been the original source of heat for the shallower

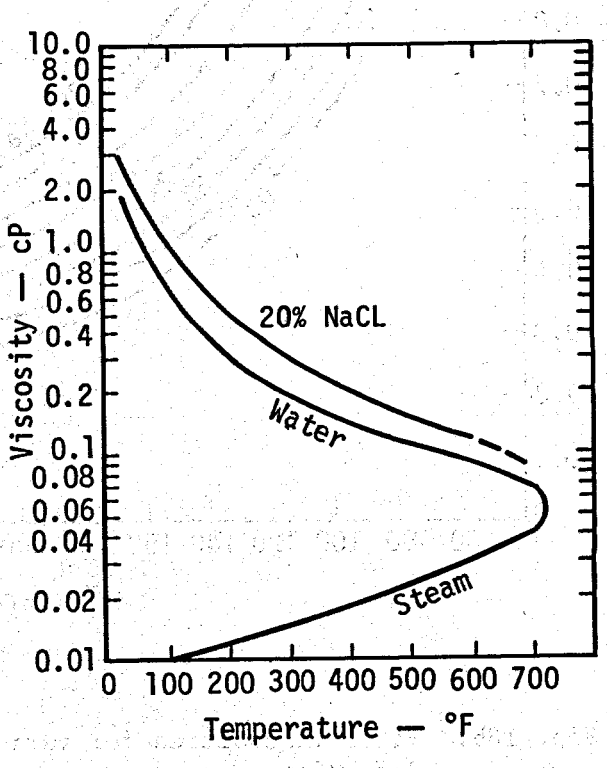

Fig. 18a. Water viscosities for a salinity and various temperatures (from Ref. 25).

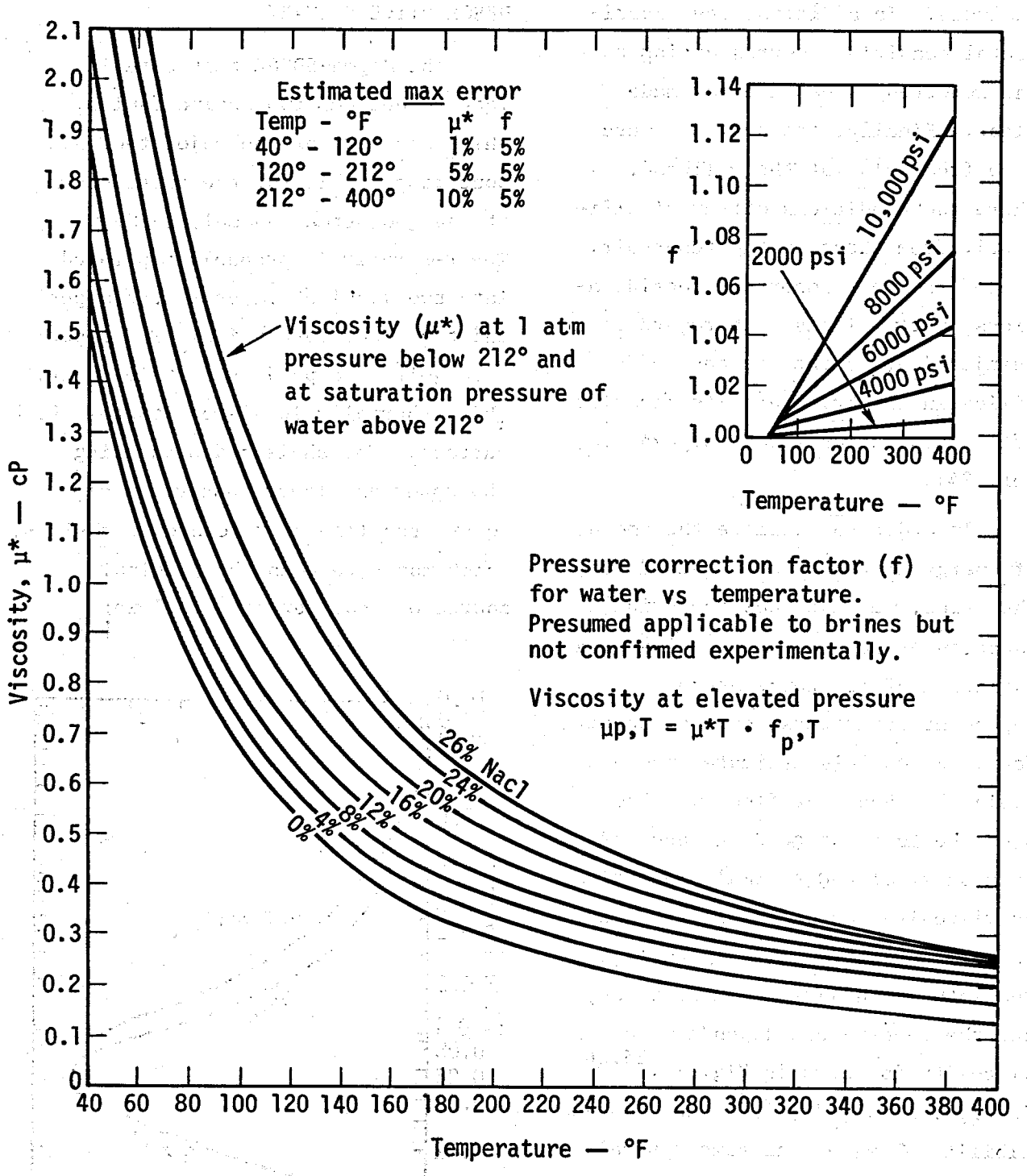

Fig. 18b. Water viscosities for various salinities and temperatures (from Ref. 26).

Fig. 19. Compressibility of water (from Ref. 25).

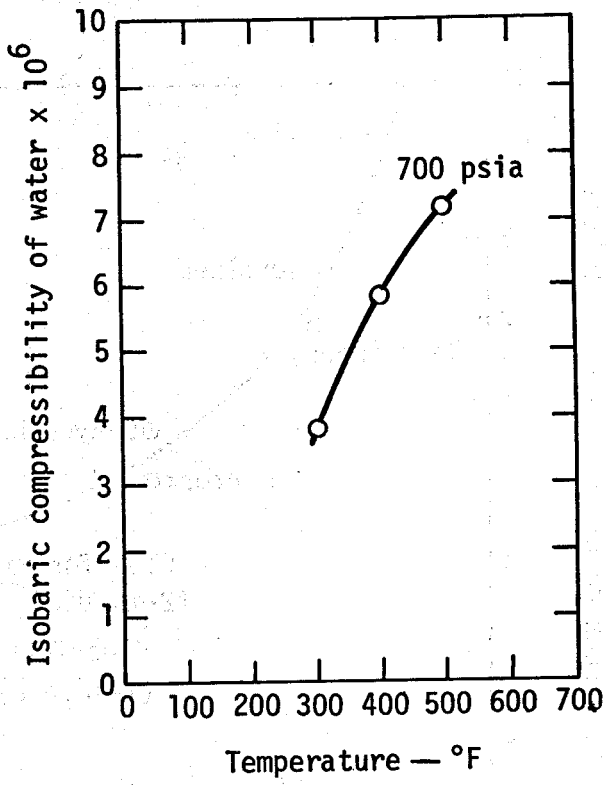

portion of the anomaly. At the Magma-SDG&E site, we estimate the total volume of the upper reservoir to be <u>at least</u> 4km^3 and the total volume of the lower reservoir to be at least 10 km^3. Other estimates for the Magma-SDG&E site, the SSGF, and the Salton Sea KGRA can be found in Refs. 7 and 20.

Fractures in the main sequence rock as inferred from cores taken elsewhere in the SSGF appear to be numerous and play a role in the flow of fluids. The reservoir's extent is probably limited only by temperature, since the rock appears to be liquid-saturated throughout the reservoir beneath the SSGF. The deep magmatic body implied by geophysical measurements is extensive and suggests that the anomaly extends out under the current Salton Sea. The brine probably contains less potentially troublesome dissolved solids in the cooler, upper reservoir than in the hotter, lower reservoir. However, the relationship between the brine's enthalpy and temperature is such that the hotter brine is more attractive for power generation, since it results in larger generating efficiency.

Additional drilling and geophysical measurements are necessary to adequately define the shape and size of the resource and the properties of the reservoir's rock and fluid. Detailed recommendations for future measurements are included in the final section of this report.

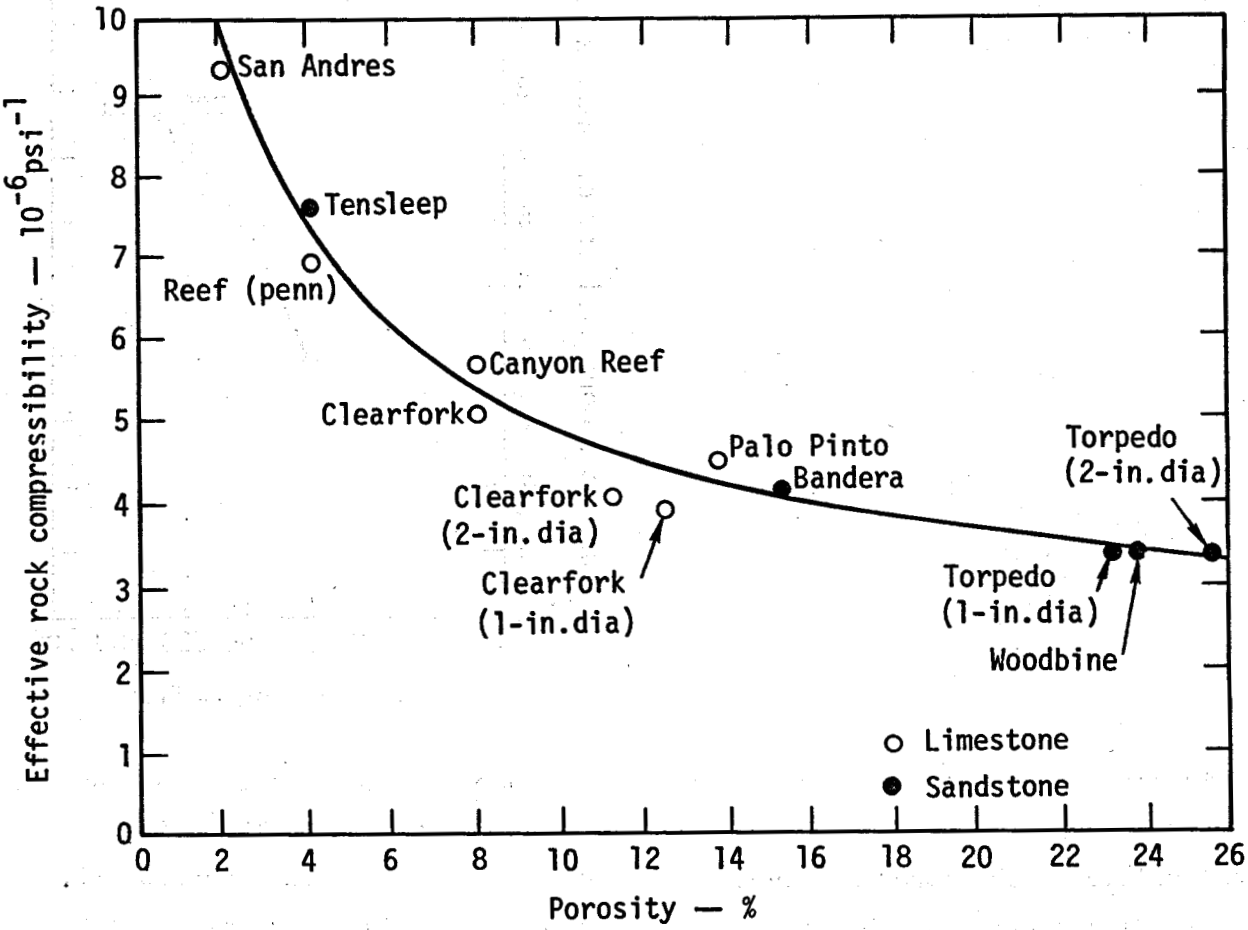

Fig. 20. Effective formation (rock) compressibility. From Ref. 27.

Reservoir Flow Characteristics

To characterize the flow patterns in a reservoir, the transmissivity (permeability) of the reservoir rock for flow of a given fluid or fluids must be determined. Permeability is a tensor quantity, requiring both magnitude and direction for a complete description. Rarely does this complete information become available during the course of reservoir analysis. The magnitude of the transmissivity provides the measure of fluid flow per unit drawdown. Directional dependence of the permeability indicates directions of restricted or enhanced flow (from a given point). However, transmissivity is usually assumed to be isotropic in the bedding plane when no information is available. In bedded sediments, the permeability in the bedding plane may often be many times that in the perpendicular direction. This is particularly true for averages over

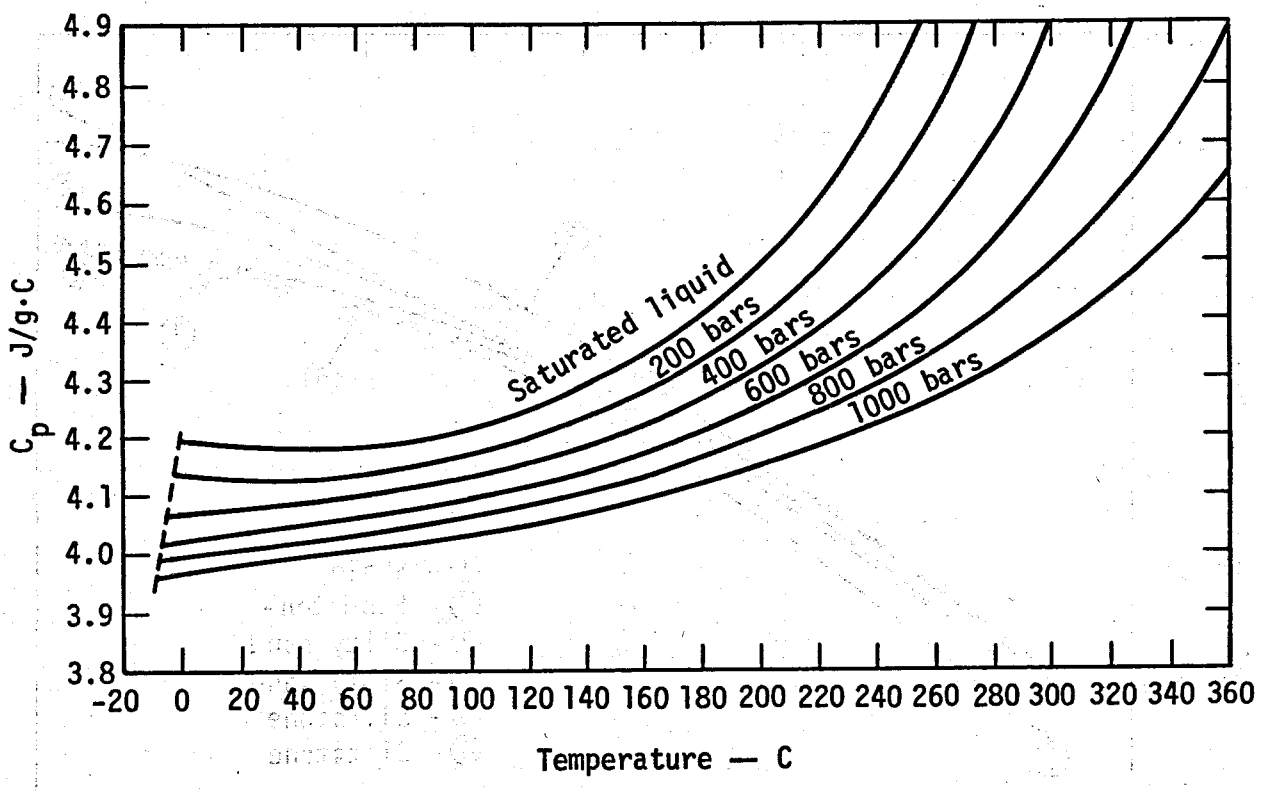

Fig. 21. Specific heat capacity of water at constant pressure $(\partial h/\partial t)_p$. Below 65°C the curves have been smoothed, as compared with calculated values, by less than one part in 250. From data in Ref. 28.

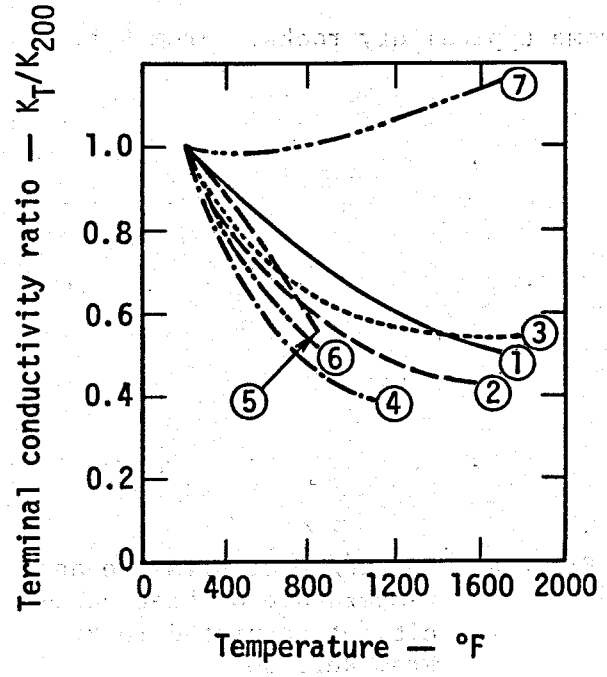

Fig. 22. Dry-rock thermal conductivity ratios: 1--bandera sandstone; 2--bera sandstone; 3--boise sandstone; 4--limestone; 5--shale; 6--rock salt; 7--tuff. From Ref. 29.

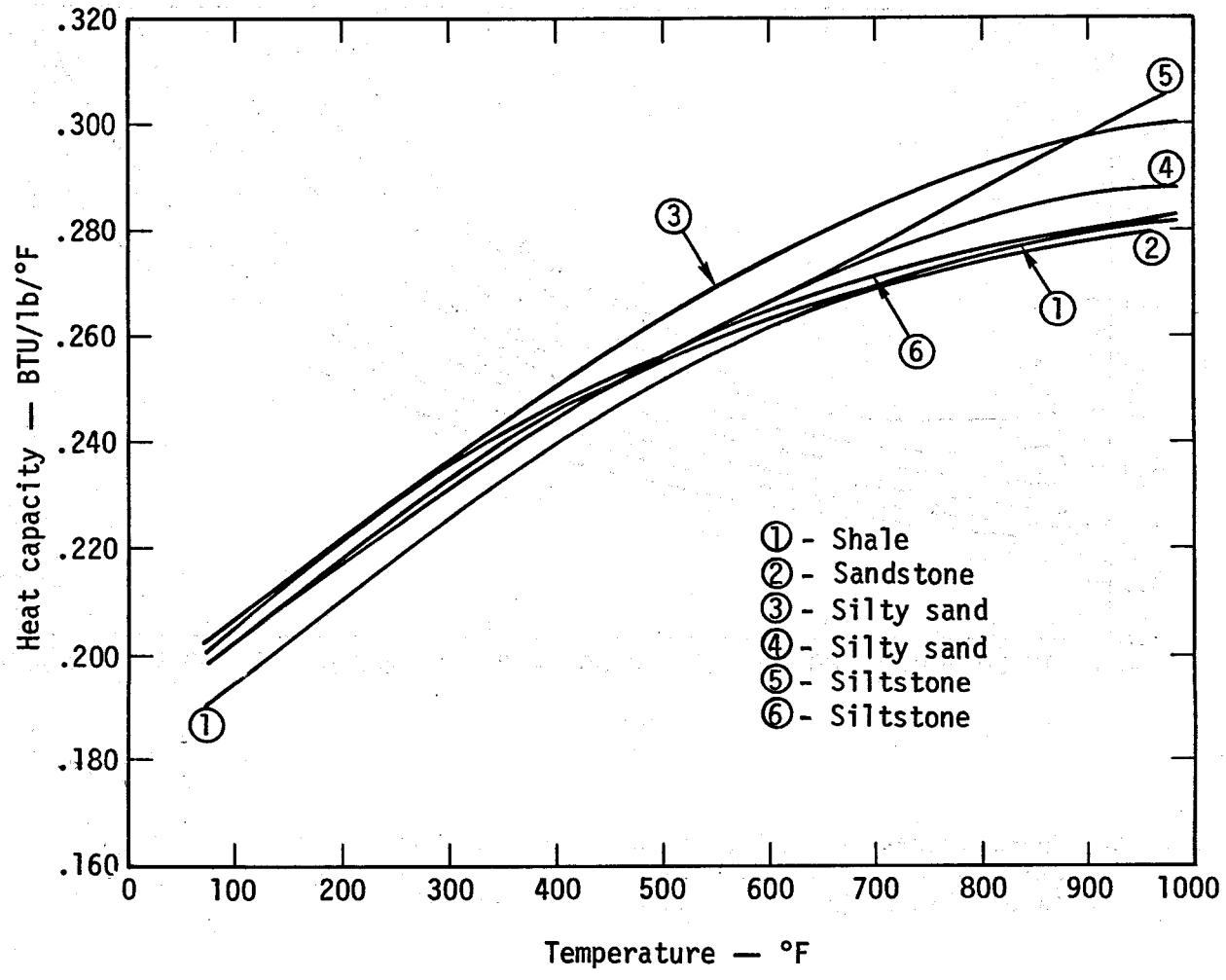

Fig. 23. Experimental heat capacities of some typical dry rocks. From Ref. 29.

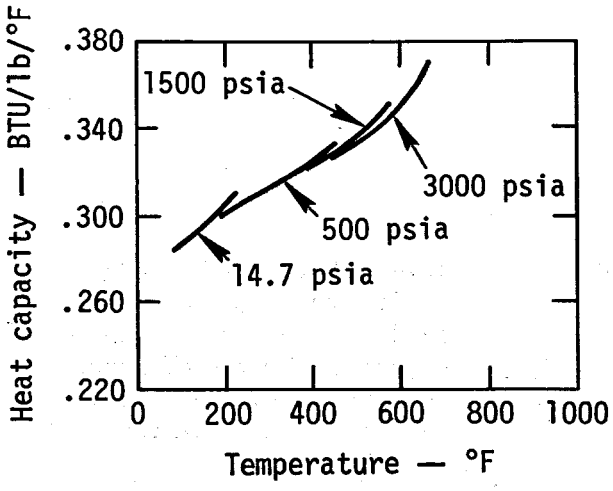

Fig. 24. Influence of pressure and temperature on heat capacity of saturated rock. From Ref. 30.

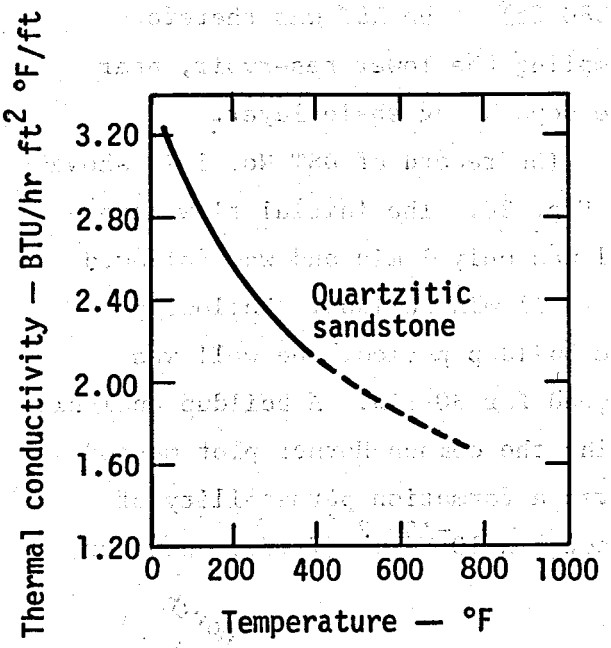

Fig. 25. Variation of thermal conductivity with temperature for saturated rocks. From Ref. 30.

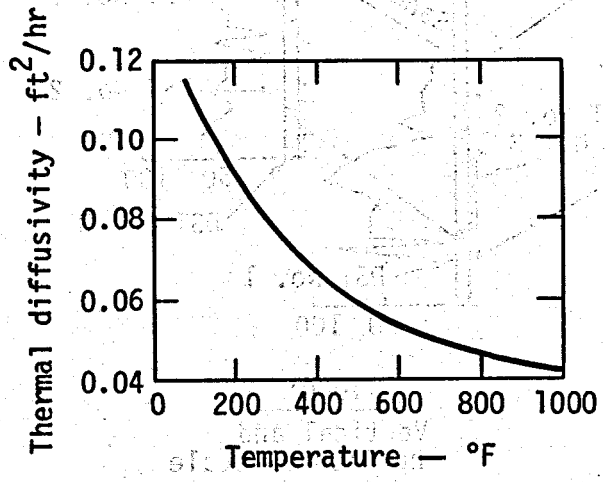

Fig. 26. Estimated thermal diffusivity of saturated quartzitic sandstone. From Ref. 30.

large distances when shale layers or lenses are present, as is the case at the SSGF.

CHARACTERISTICS OBTAINED FROM DRILLSTEM TESTS

We have obtained and analyzed drillstem test (DST) records for two of the Magma-SDG&E wells — Magmamax No. 1. and Woolsey No. 1. In each well, three DST's were recorded when the wells were drilled. In all cases, the DST showed equalization when the well was flowed for more than a few minutes. Equalization occurs when the formation's permeability and storage are large [31] and is characterized by a return of the downhole pressure to nearly the hydrostatic-reservoir pressure during extended flow periods. In oil and gas DST's, the flow periods and shut-in times are often several hours, days, or longer. In these geothermal well tests, the DST was completed within about an hour.

Magmamax No. 1

For the Magmamax No. 1 well, three DST's were recorded during drilling, but only the first DST record allowed quanitative analysis for transmissivity. In the remaining two tests, equalization occurred so fast that such analysis was not possible.

The well was initially drilled nonstop to 802.2 m (2632 ft). For DST No. 1, the packers were set at 781.5 m (2564 ft) and 779.1 m (2556 ft), providing 2.4 m (8 ft) flow interval. In Fig. 27, the electric log correlation of Towse[7] is shown, where the approximate depths of the DST's are denoted by arrows. DST No. 1 was carried out at about 780 m (2560 ft) and the shale bed reported in Towse[7] is at about 725.4 m (2380 ft). The DST was therefore sampling the lower reservoir, near the separating shale layer.

The record of DST No. 1 is shown in Fig. 28. The initial flow interval was only 1 min and was followed by an 11-min buildup. Following the buildup period, the well was flowed for 30 min. A buildup analysis using the common Horner plot method gives a formation permeability of about 7×10^{-15} m^2 (7 md). However,

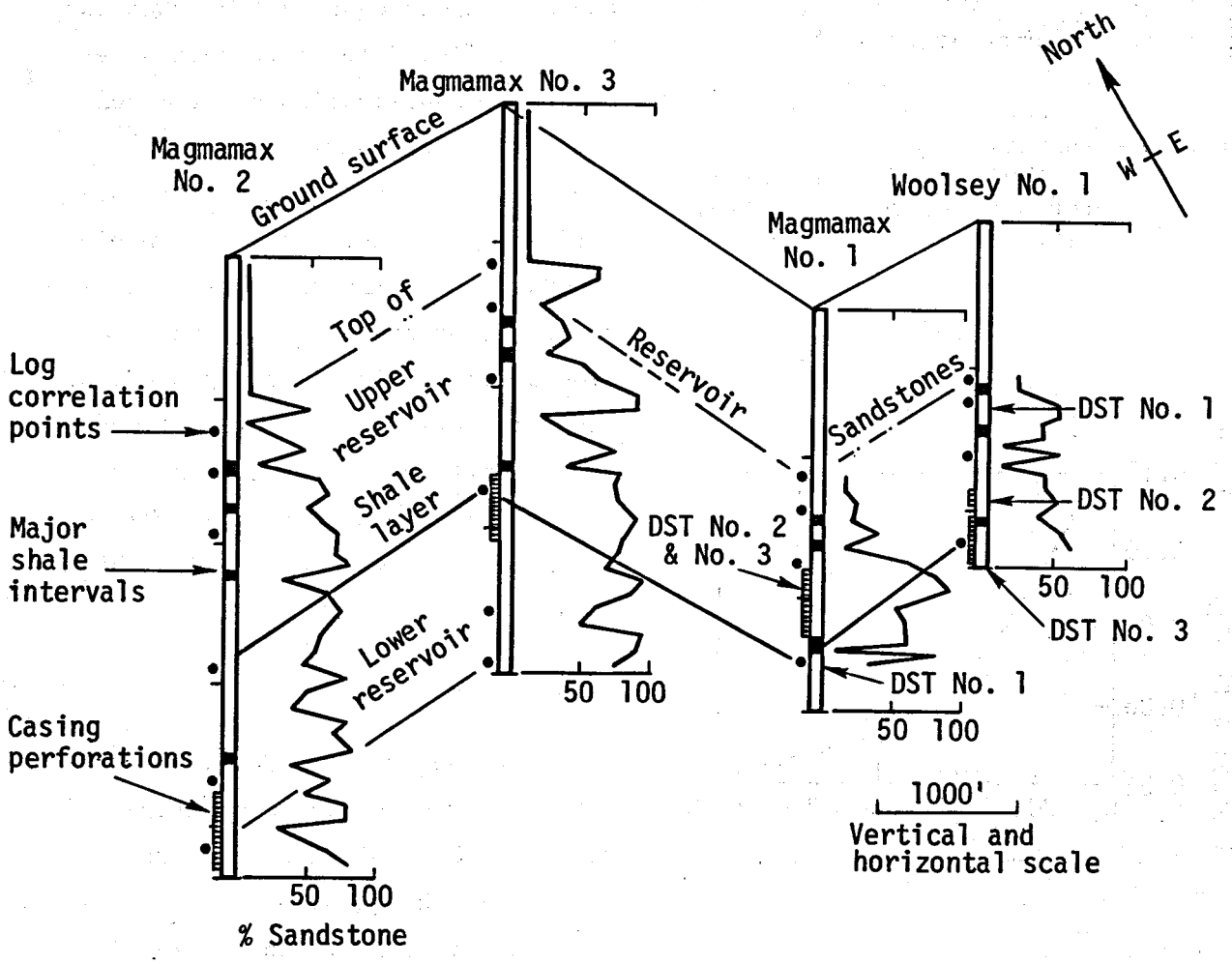

Fig. 27. Electric log analysis at the Magma-SDG&E geothermal test site. The wells are shown in oblique projection (horizontal and vertical dimensions are true). Jagged lines along wells give percent sandstone at that depth. Information from D. Towse, 1-5-76.

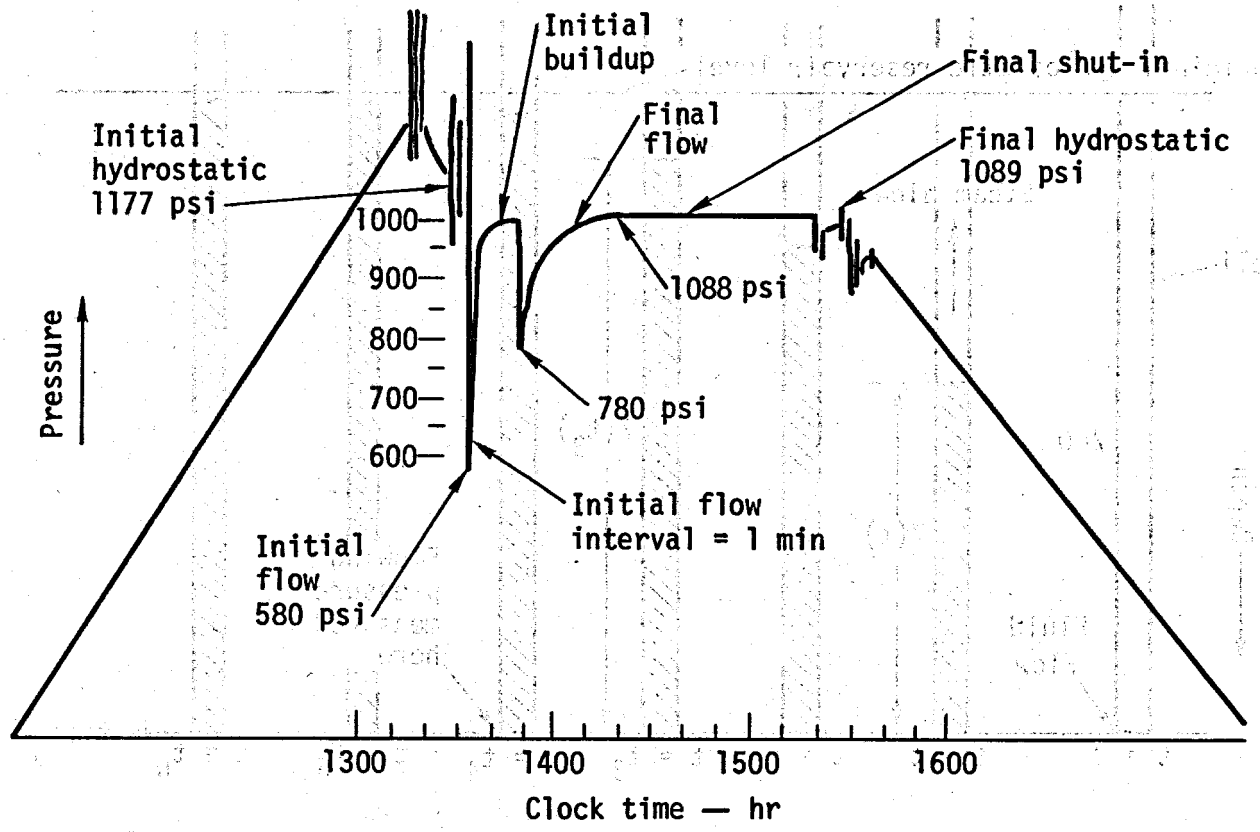

Fig. 28. The record of the first drillstem test in the Magmamax No. 1 well. The depth of the test was 802 m (2632 ft).

this result is not reliable, since the initial flow period (immediately following drilling) was too short for the well to stabilize and was probably too short for the flow to remove the cake built up during drilling.

This leaves the 30-min drawdown of DST No. 1 to be analyzed. The driller's record indicates "a moderate steam blow decreasing to nothing during the flow period". No liquid from the well was noted. Such a flow test with equalization can be qualitatively pictured as in Fig. 29. The DST tool is opened, with an accompanying pressure drop in the formation. At time t = o, the fluid begins to fill the drillstem. During the equalization, some steam blows off.

To estimate the formation's permeability, we will first determine the time-dependent flow rate during drillstem fillup, using the model shown in Fig. 29. Then we will use a multirate analysis of the DST No. 1 data from Fig. 28 to get the value of transmissivity.

If Z is the height of the column of liquid and s is the head; then, neglecting friction, well-bore heat loss, etc.

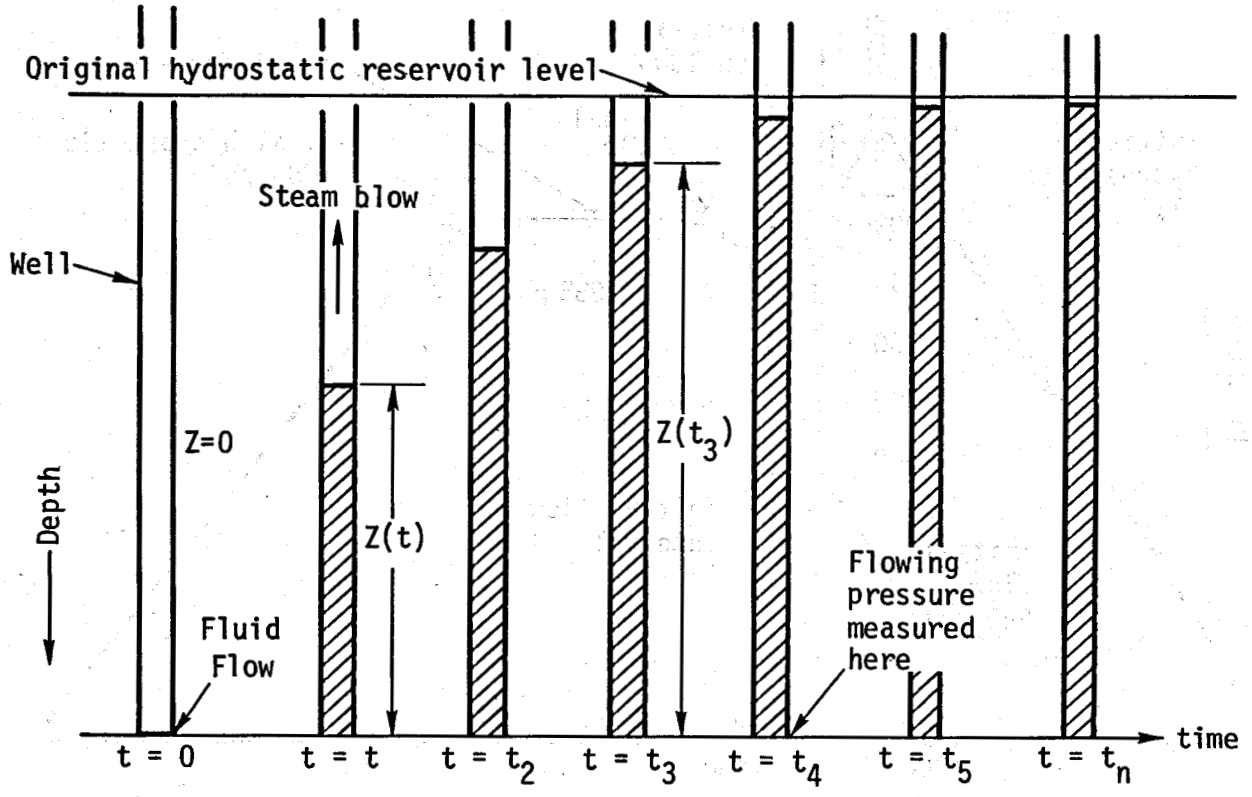

Fig. 29. Model used to estimate transmissivity of reservoir formation from DST data. The horizontal bars in the wells at different times show the level of the liquid as a function of time as the fluid flows into the drillstem at the point corresponding to t = 0.

$$\frac{ds}{dt} = \rho g \frac{dZ}{dt} = \frac{g}{A}(q - q_s) \qquad (1)$$

where q_s is the mass flow rate of the steam, q is the total mass flow rate, and A is the drillstem's cross-sectional area. Using x as the steam quality, we have the time-dependent mass flow rate, q(t) given by

$$q(t) = \frac{A}{g(1-x(t))} \frac{ds(t)}{dt}$$

$$\approx \frac{A}{g}\left[\frac{1}{(1-x)} \frac{\Delta s}{\Delta t}\right] . \qquad (2)$$

The driller's record from Magmamax No. 1 reports the steam blow declined to zero, and for simplicity we assume a linear decrease from an initial value of $x(0) \approx 0.18$. The superposition principle gives the transmissivity for a multirate analysis as[26]

$$\frac{kh}{\mu} = \frac{1}{(2\pi\rho)} \qquad (3)$$

$$\cdot \frac{\sum_{i=1}^{N} \left[(q_i - q_{i-1}) P_D \left(1, t_{Di} - t_{Di-1}\right)\right]}{(P_{initial} - P_{r_w, t_{DN}})} .$$

The flow interval is h, the well radius is r_w, and P_D is the dimensionless drawdown function. The initial

mass flow rate is defined to be $q_0 = 0$, and the dimensionless time is

$$t_D = \frac{\lambda t}{r^2} \quad . \qquad (4)$$

Here, λ is the diffusivity:

$$\lambda = \frac{k}{\phi\mu\beta} \quad (\text{in } m^2/s). \qquad (5)$$

In these equations,

$P_{initial}$ = initial hydrostatic pressure (in Pa);

$P_{r_w, t_{DN}}$ = pressure at radius r_w at time t_{DN};

ϕ = porosity;

μ = viscosity (in Pa·s);

β = compressibility (in Pa^{-1}).

We assume P_D to be a line source in an infinite reservoir. Then the dimensionless pressure drop P_D is approximated by

$$P_D\,(r/r_w,\ t_D) = 1/2\ \ln(4\lambda t/\gamma r^2) \qquad (6)$$

where γ is Euler's constant $\approx$ 1.78. In Table 3, the appropriate values of these parameters, obtained from the first DST in the Magmamax No. 1 well, are given.

The permeabilities calculated from these parameters are shown with the corresponding incremental mass-flow rates in Fig. 30. The permeability stabilizes at about 160 md. The corresponding transmissivity is about 3.25×10^{-13} $(m^3/s)/Pa$.

The assumed value for permeability, which is used in calculating

Table 3. The estimated parameters for interpreting DST No. 1 in the Magamamax No. 1 well.

Symbol	In metric units		In English units	
	Value	Units	Value	Units
r_w	0.028575	m	2.25	in.
ϕ	0.2			
μ	1.2×10^{-4}	Pa·s	0.12	cP
β	6.2×10^{-10}	Pa^{-1}	4.4×10^{-6}	psi
ρ	1000	kg/m^3		
h	2.43	m	8	ft
$k_{assumed}$	1.6×10^{-13}	m^2	160	md

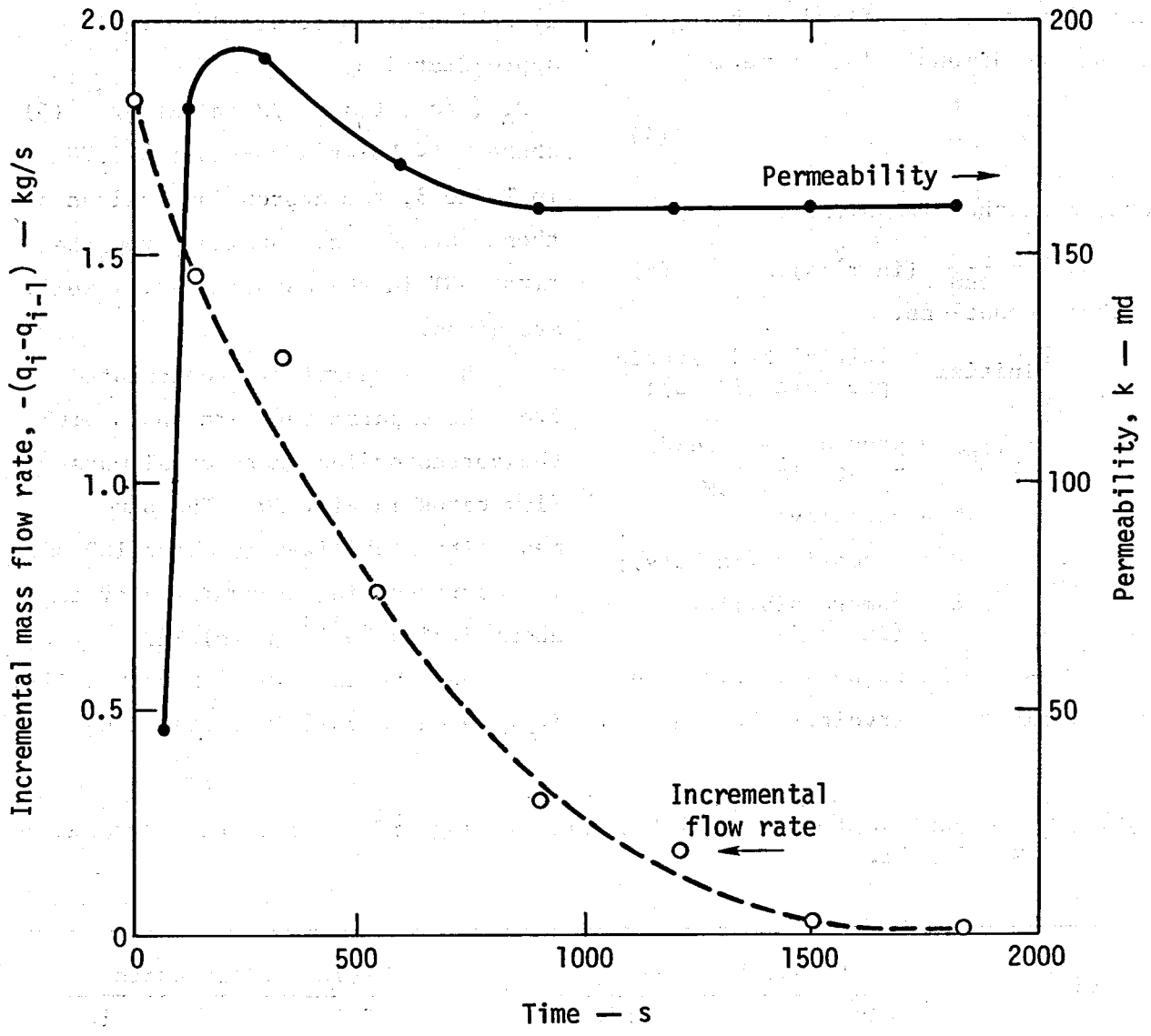

Fig. 30. The incremental flow rates and permeabilities from the Magmamax No. 1 well, DST No. 1, obtained during flow equalization. The dashed line gives the flow-rate increments, with the scale at the left, and the solid line gives the permeabilities, with the scale at the right.

the diffusivity, and hence the line-source type-function is not fortuitous. The k value of about 160 md was obtained by iterating until the permeability resulting from the drawdown analysis agreed with the assumed permeability in the diffusivity.

In the first DST at the Magmamax No. 1 well, the interval sampled is quite small (2.4 m, or 8 ft), and one might argue that the test was really sampling a much greater section of the reservoir. However, we note again that the test was made very close to the thick shale layer separating the

upper and lower reservoirs. From this, we can conclude that the test only sampled below the upper packer — in the lower reservoir — since near the shale we would expect very little vertical permeability.

Another consideration is the effect of the choices of parameters on the resulting value of permeability. The drillstem's radius can be assumed to be exact and, since the values of ϕ and β appear only in the diffusivity, the product $\phi\mu\beta$ will change the permeability less than 10% when the product varies by a factor of two (for the time intervals considered here). The only remaining parameter that can affect the result is ρ, and we consider the value $\rho = 1000\ kg/m^3$ correct to about 5% (see for example Ref. 17)

The driller's records for Magmamax No. 1 show that immediately after DST No. 1, the hole was backfilled with cement to 558.7 m (1833 ft) to combat fall-in. After drilling out the cement to 588.3 m (1930 ft), the second and third DST's were run. DST No. 2 produced about 15 gal/min for eight minutes, according to the driller's log. Fig. 27 shows that the second and third DST's in Magmamax No. 1 were made in the prime sand of the upper reservoir. The DST No. 2 record shows that equalization occurred within eight minutes after the initial drawdown. This implies much higher permeabilities than we have calculated for the lower reservoir near the shale layer. DST No. 3 was taken following mud reconditioning and showed slower equalization (as might be expected) because of skin formed during reconditioning. Even with the skin, the permeability appears much higher than measured from DST No. 1. The equalizations of both DST No. 2 and DST No. 3 were too rapid to allow any quantitative estimate of transmissivity from the data.

Woolsey No. 1

Three DST's were run during the drilling of the Woolsey No. 1 well. The first test was made at about 393.3 m (1290 ft) with the packers at 392.1 m (1286 ft) and 394.4 m (1294 ft). The open interval is again about 2.4 m (8 ft). During both the buildup following a two-minute flow interval and the final 30-minute flow interval, the well equalized extremely rapidly, allowing no analysis of DST No. 1 at all. We can only conclude from DST No. 1 that the permeability around the Woolsey No. 1 well in the upper reservoir at about 375 m (1230 ft) is very large and is similar to the permeability around the Magmamax No. 1 well in the upper reservoir at about 575 m (1890 ft).

The second DST at the Woolsey No. 1 well was carried out after the well was drilled to 602.6 m (1977 ft). The packers were set at 583.1 and 581.3 m (1913 and 1907 ft), for an open interval of about 2.2 m (6 ft). The well showed "medium blow decreasing to faint blow". The well was flowed for one hour; no buildup was recorded. From Fig. 27, we see that DST No. 2 took place in the upper reservoir but quite close to the shale layer — located between 610 m and 640 m (2000 and 2100 ft) — separating the reservoir.

Figure 31 is the record of DST No. 2. This record was analyzed by the same method as was the first DST of the Magmamax No. 1 well. In Fig. 32, the permeabilities computed from the analysis are plotted. The parameters used in the computations were the same as in Table 3, except for the iteratively determined value

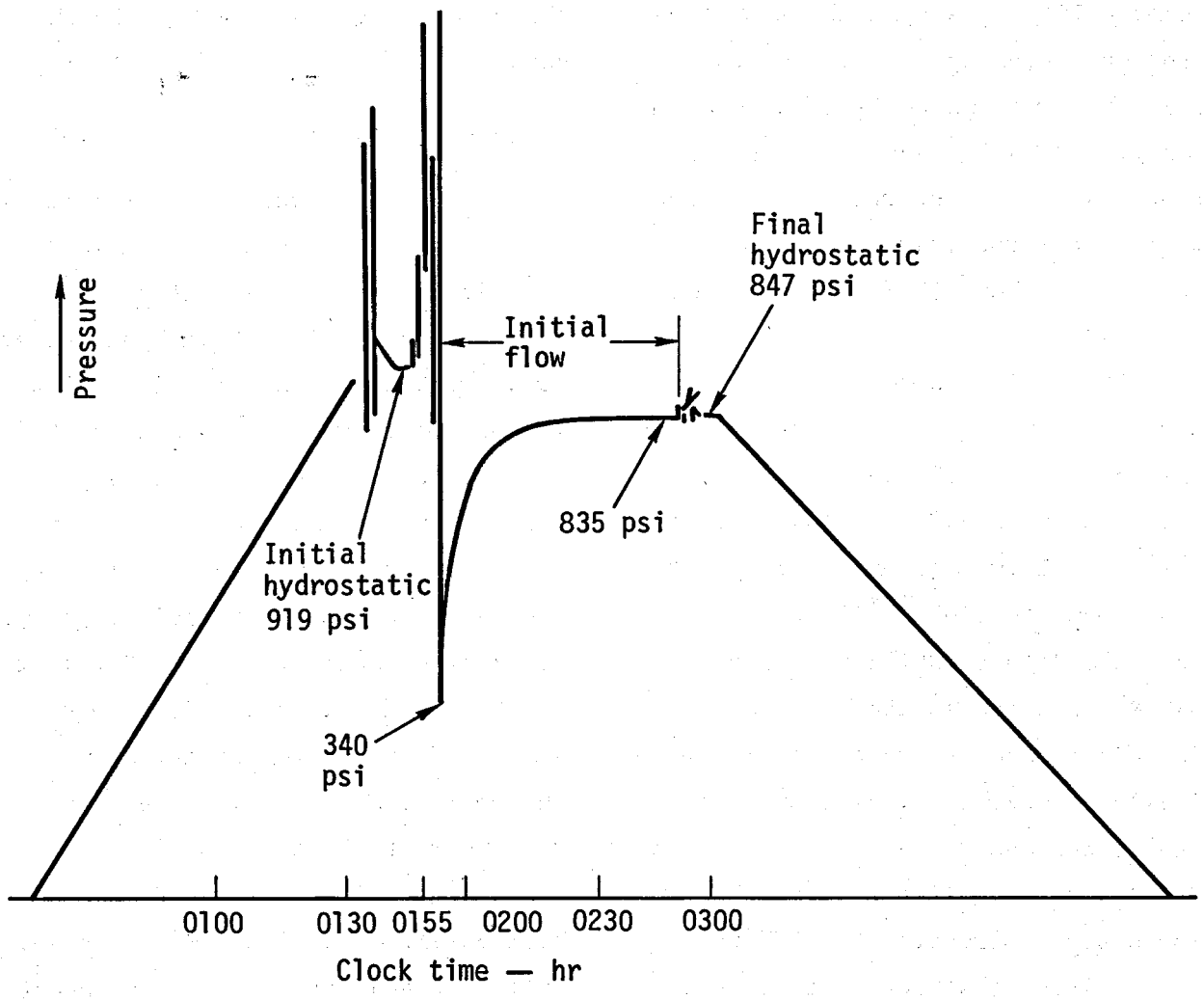

Fig. 31. The Woolsey No. 1, DST No. 2 taken at 603 m (1977 ft).

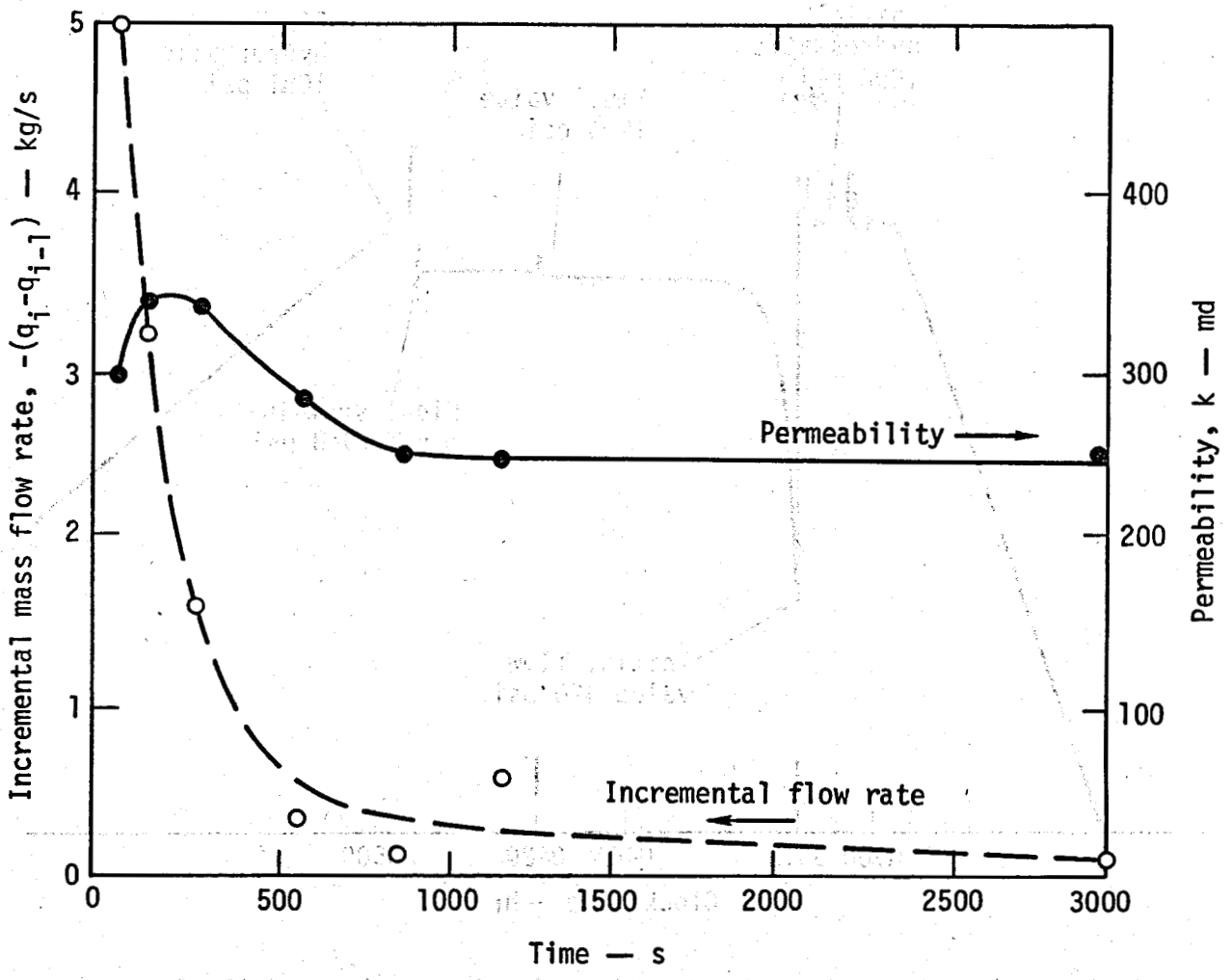

Fig. 32. The incremental flow rates and permeabilities from the Woolsey No. 1 well, DST No. 2. The dashed line gives the flow rates, with the scale at the left. The solid line gives the permeabilities, with the scale on the right.

of permeability, $k \approx 247$ md, which was used in the line-source, type-curve function. The corresponding DST transmissivity is about 4.5×10^{-13} $(m^3/s)/Pa$.

Figure 33 is the record of the third DST performed at the Woolsey No. 1 well. This DST was performed after the well was drilled to 732 m (2400 ft). Hence, it provides us with data to analyze the lower reservoir. Figure 34 shows the permeabilities obtained from the DST record. Analysis was not made at early times because of the presence of an apparent skin. The skin effect is present in the plot in Fig. 31 of the mass flow rate (not flow rate increment), which shows an initial increase in flow rate as the drawdown decreases during drillstem fillup. The resulting value, $k \approx 177$ md, is similar to the

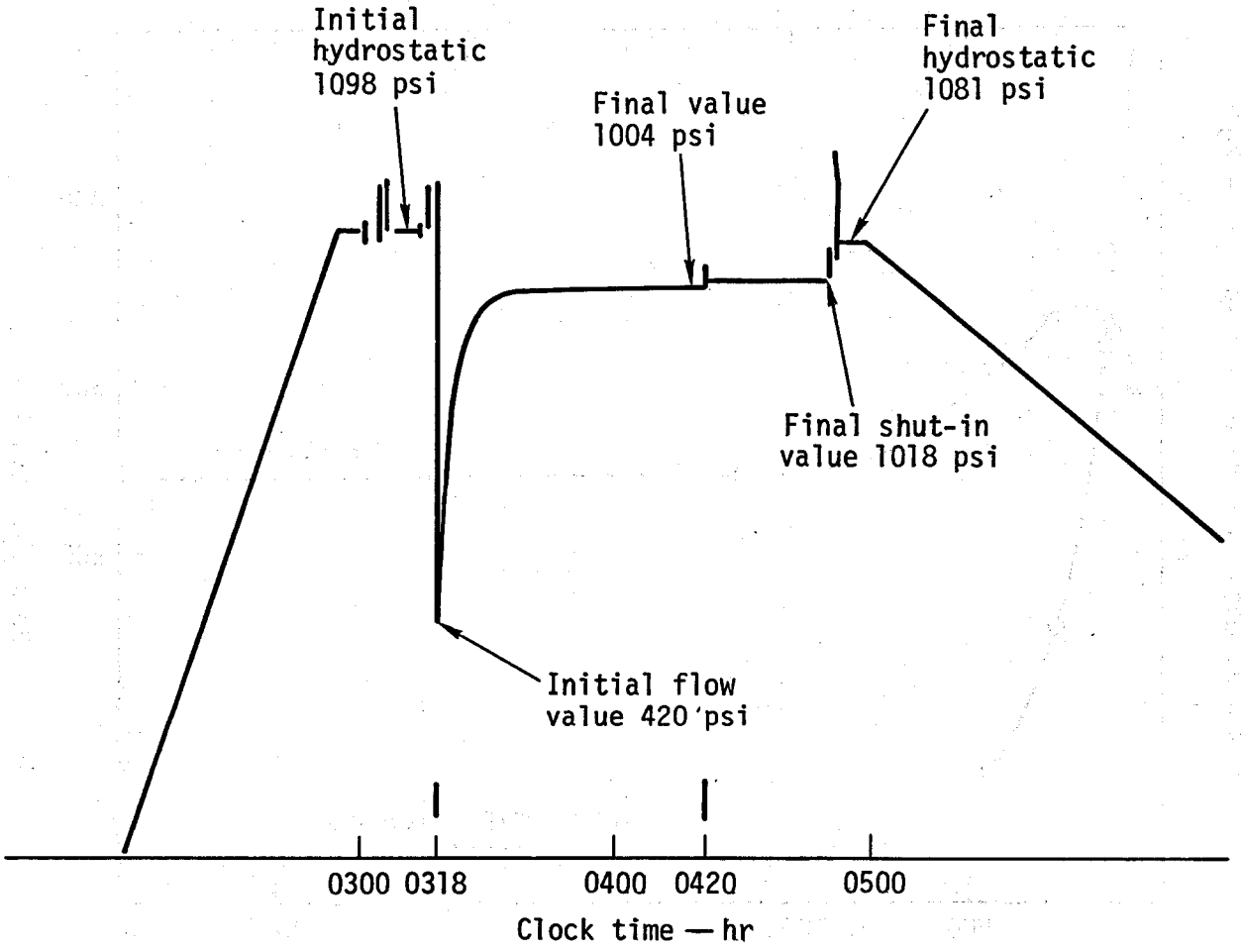

Fig. 33. The Woolsey No. 1 DST No. 3 taken at 732 m (2400 ft).

result $k \approx 160$ md, obtained from the first DST of the Magmamax No. 1 well at approximately the same depth.

We can summarize our analyses of the DST's for these two Magma-SDG&E wells as follows.

- The permeability of most upper reservoir sands is very high. The values probably exceed 500 md, and the sands have high porosity — 30%. or more.[19]
- However, in the upper reservoir, near the shale layer that separates it from the lower reservoir, the permeability is probably less than 250 md, and there is probably very little vertical permeability. The porosity in this area is much lower — less than 20%.
- In the lower reservoir, near the shale layer, the permeability is between 150 and 200 md, and the porosity is about 20%.
- Saraband analyses[19] at Magmamax No. 2 and Magmamax No. 3 support these findings for the Magma-SDG&E

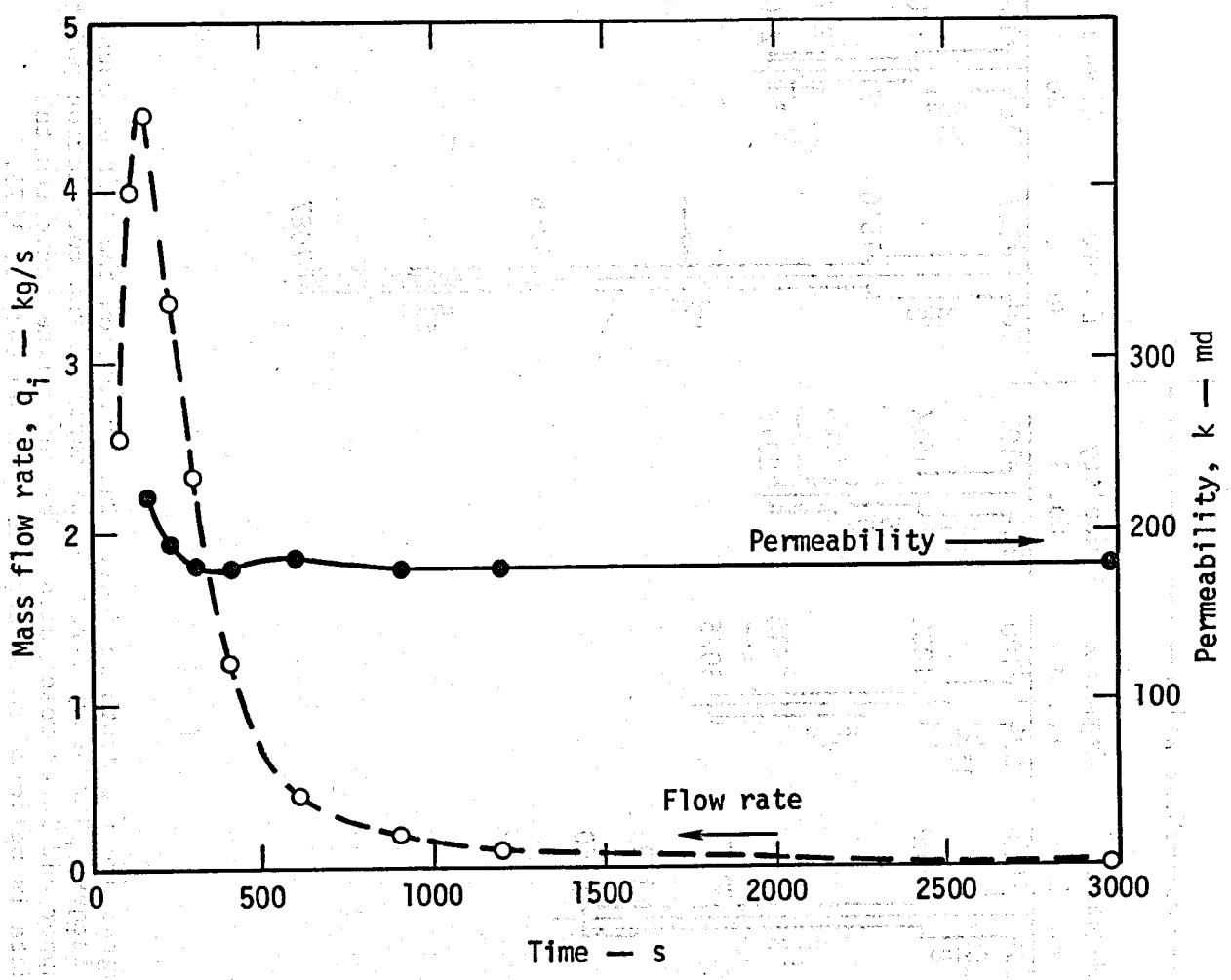

Fig. 34. The mass flow rate, given by the dashed line and left scale, and the permeability, given by the solid line and right scale. Data is from DST No. 3 at the Woolsey No. 1 well.

reservoir down to about 820 m (2700 ft). However, below this depth the Saraband analysis indicates less porosity and lower permeability at these wells.

CHARACTERISTICS OBTAINED FROM WELL-FLOW TESTS

One of the major problems limiting our reservoir assessment and production extrapolation is the lack of sufficient well-production data. Most of the meager data that exist are currently held confidential. However, this is not an unusual situation in reservoir studies. Fortunately, we do have some information about the Magma-SDG&E wells and some of their nearest neighbor wells.

Magmamax No. 1 production test

The Magmamax No. 1 well was completed as shown in Fig. 35. The 8-5/8-in. casing has a slotted section

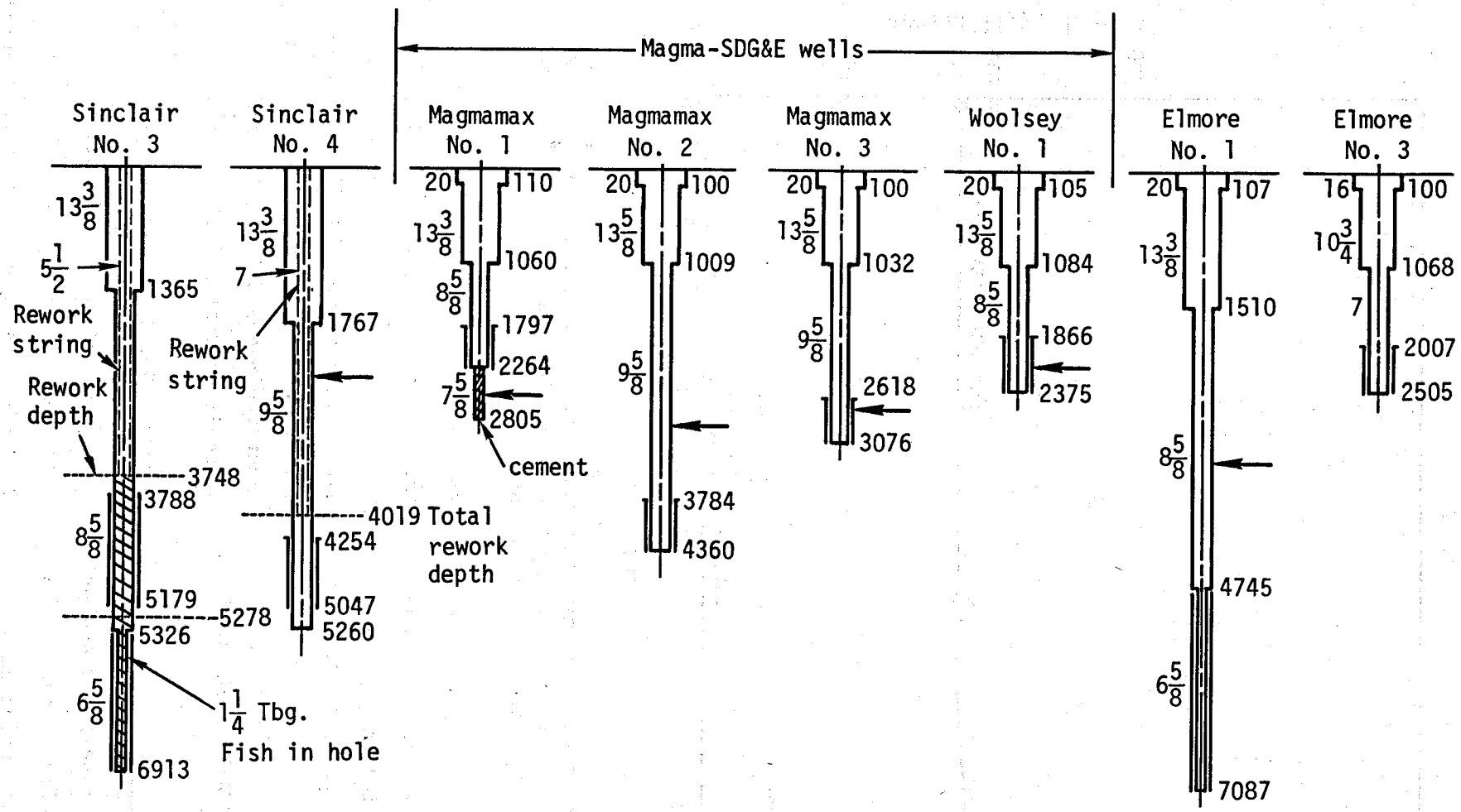

Fig. 35. The numbers on the right of each diagram are the depth in feet. The numbers on the left of each diagram are the casing diameters in inches. The heavy arrow is the depth of the correlation point for the shale break separating the upper and lower reservoirs. The heavy line indicates the location of the perforations. All data is believed to be current up to January 1, 1975.

from 547.7 m (1797 ft) to 690.1 m (2264 ft). The well was tested for one week in 1972. Unfortunately, we do not have a detailed description of the test. In Fig. 36, the reported wellhead temperatures, wellhead pressures and mass flow rates are plotted as a function of time. This test was carried out with a constant orifice size of 8 in. Although the wellhead pressure and temperature appear to have been stabilizing near the end of the test, the flow rate does not.

From the location of the casing's perforations (the slots) and the location of the shale break (see Fig. 35), we see that Magmamax No. 1 draws entirely from the upper reservoir if no fracture permeability provides vertical communication across the shale layer. Determining permeability from the model of Eqs. (3) to (6) requires that we know two variables as a function of time: flow rate and downhole pressure. The downhole pressures were not reported for this well test; only the wellhead pressures are known. Hence, we are left with two ways to estimate the permeability. One is to simulate the two-phase wellbore flow and, from a complicated series of calculations, estimate permeability by matching the flow rate and wellhead conditions. The other is to take advantage of the DST information. The latter approach is much simpler.

We note that the second and third DST's in Magmamax No. 1 were carried out in the region of the perforations. Figure 37 shows drawdowns for assumed values of permeability, calculated from flow rates shown in Fig. 36. These calculations are based on the multirate model previously described. Although the drawdown is likely to be greater in the week-long well test than in the one-hour DST, in the first day of the longer test it should only be a few percent greater in strata of equal permeability. Hence, we can conclude from Fig. 37 that, in the upper reservoir, the average permeability in the major sand sequence exceeds 5×10^{-13} m^2 (500 md). The corresponding transmissivity in the perforated section exceeds 5×10^{-7} $(m^3/s)/Pa$.

Injection tests

Fresh-water injection tests were carried out on Magmamax No. 2 and No. 3 and Elmore No. 3 immediately following well completion. Magmamax No. 2 is completed with perforations in the lower reservoir. Magmamax No. 3 is completed with perforations probably just below the shale layer separating the upper and lower reservoirs, as shown in Fig. 35.

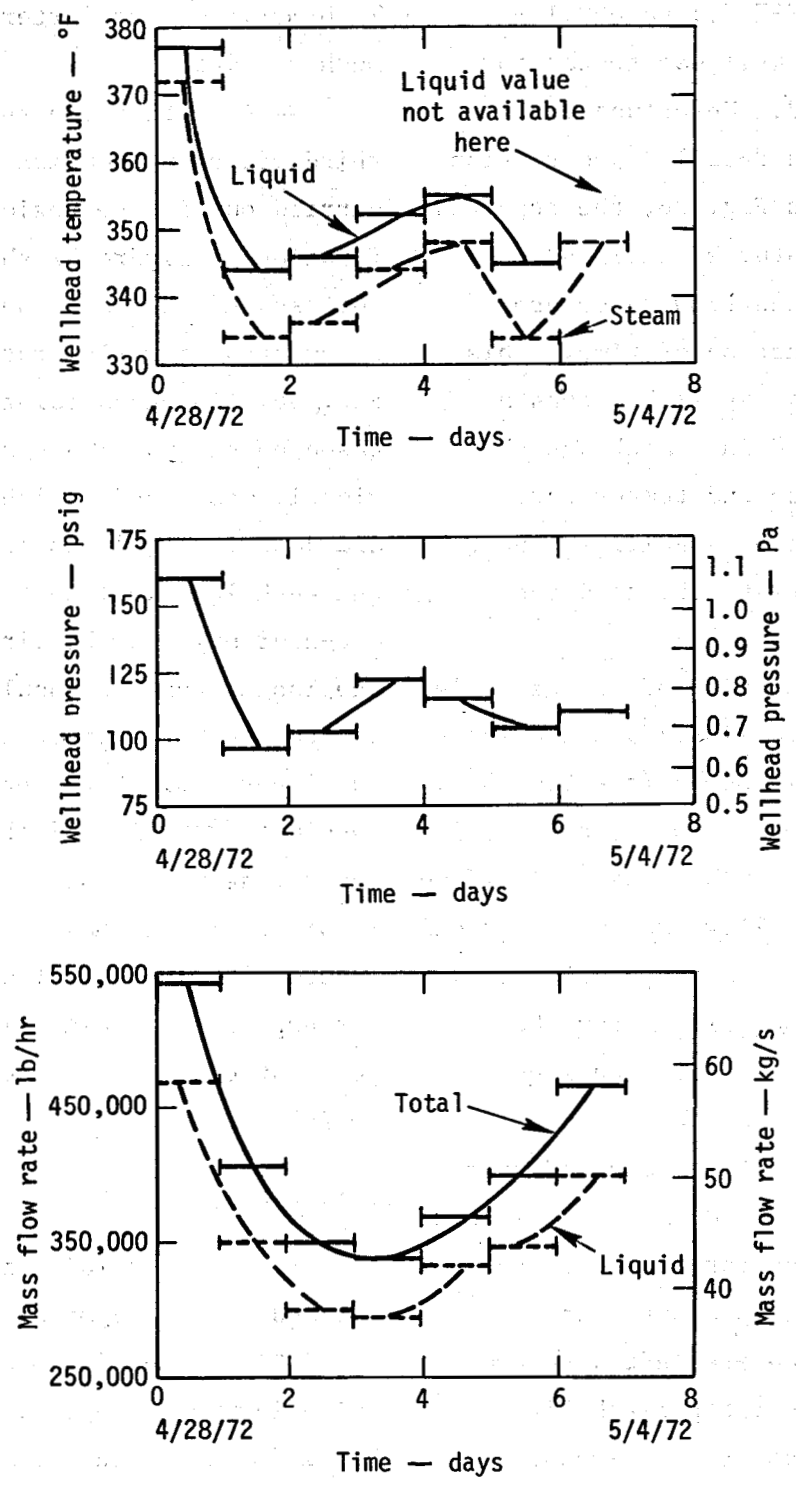

Fig. 36. Magmamax No. 1 production history during a one-week period in 1972.

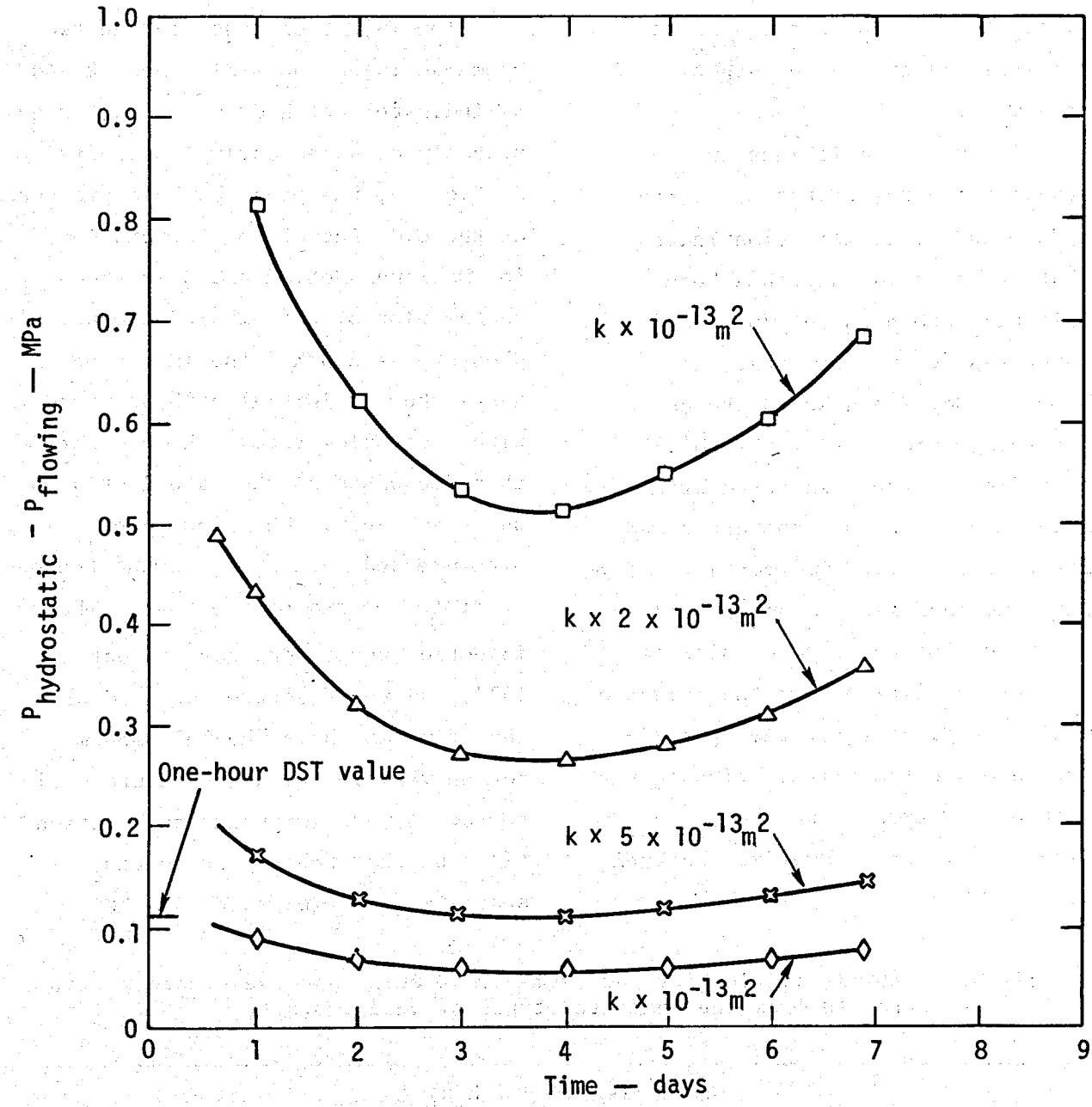

Fig. 37. Drawdown during the one-week Magmamax No. 1 well test for different values of average formation permeability. The drawdown value obtained during the one-hour DST's are shown for comparison (1 Darcy = 10^{-12} m^2, 1 MPa = 10^6 Pa = 145 psi).

Elmore No. 3 is perforated above the shale layer, in the upper reservoir.

The well completions and a study of the temperature vs depth before and after injection indicate that fresh, cold water has been injected into both the upper and lower reservoirs, and that, if Magmamax No. 2 and No. 3 are used for reinjection during the SDG&E experiments, the reinjected brine might appear in both the upper and lower reservoirs. Rudimentary analyses have been carried out to give estimates for the transmissivities and permeabilities near the injection wells. Estimates for the approximate average transmissivities in the completed Magmamax, Woolsey, and Elmore wells are summarized in Table 4.

The injection tests in the two Magmamax injection wells (Nos. 2 and 3) indicate that hydraulic fracturing probably occurred during the tests. In Fig. 38, the peak downhole pressure at the midpoint of the perforations for Magmamax Nos. 2 and 3 is shown on the plot of bottomhole fracturing pressure vs depth. The injection tests show an initial high pressure with a low flow rate. The pressure then decreases as the rate increases quite suddenly. The subsequent pressure and rate are constant thereafter to the end of the test. These injection tests were carried out in 1972, and the fractures created at that time may have "healed" and may not be very important in future well tests. A more important observation might be that the injection tests stabilize--at flow rates on the

Table 4. Transmissivities for the Magma-SDG&E wells and the Elmore wells, obtained from the indicated types of well tests.

Well	Transmissivity (kh/μ), $(m^3/s)/Pa$	Type of well test
Magmamax No. 1	$>5 \times 10^{-7}$	DST and production
Magmamax No. 2	$\approx 5 \times 10^{-8}$	Injection
Magmamax No. 3	$\approx 2 \times 10^{-8}$	Injection
Woolsey No. 1	$\approx 1.5 \times 10^{-7}$	DST
Elmore No. 3	$>2 \times 10^{-7}$	Injection
Elmore No. 1	$<5 \times 10^{-8}$	Estimated from k=50 md

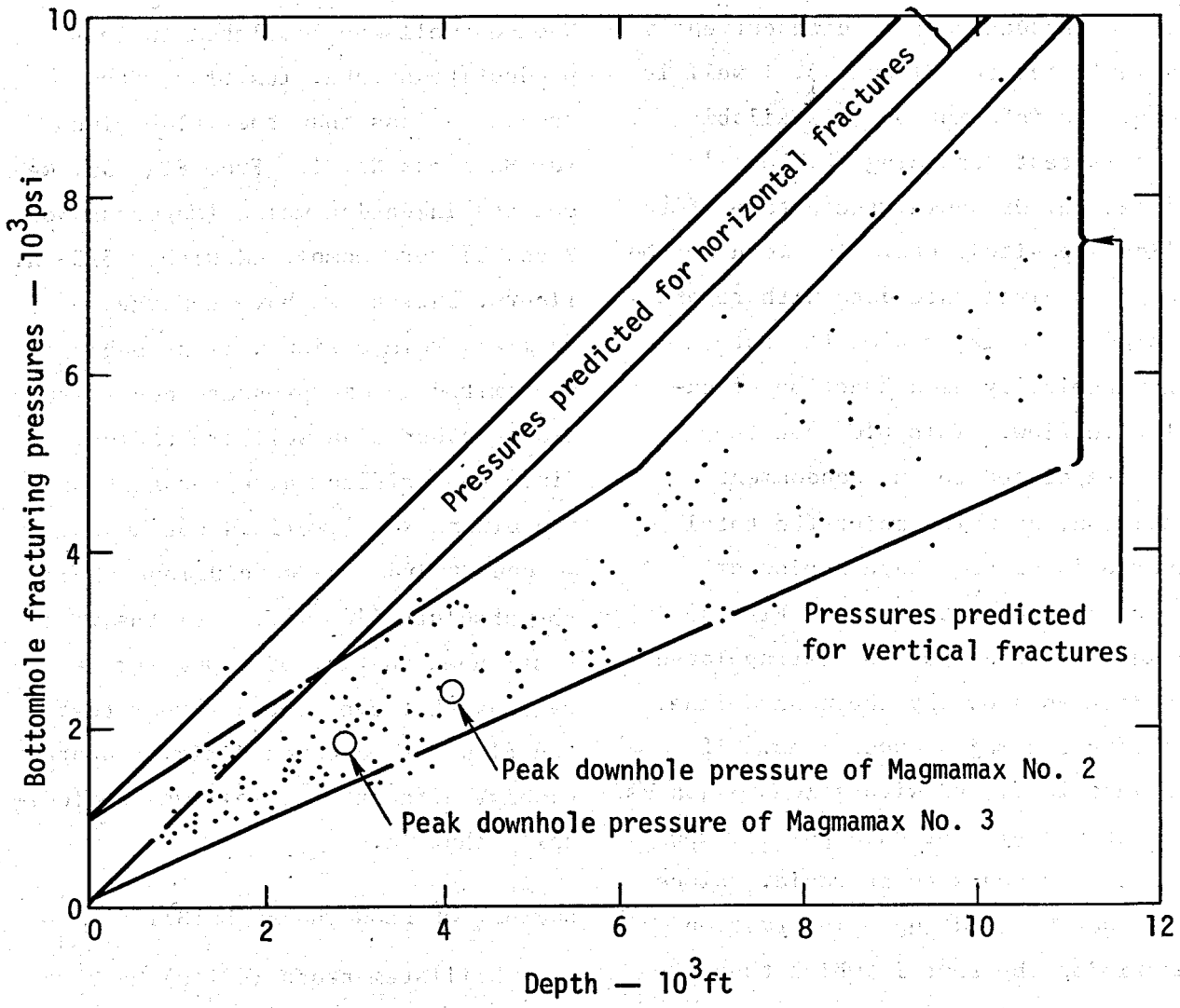

Fig. 38. Theoretically predicted bottomhole fracturing pressures and field data from Ref. 32. The experimental peak downhole pressures for the Magmamax wells are shown by the open circles.

order of 28 kg/s (225 000 lb/h), and an over-pressure between 1.38 and 2.25 MPa (200 and 350 psi, respectively). These values were observed in the Magmamax No. 2 and No. 3 and the Elmore No. 3 injection tests, and indicate the approximate minimum pressure required for reinjection.

The Sinclair No. 3 well was produced for one day in 1963, but there is insufficient data from it to calculate permeability. In 1973, the well was reworked and an injection test was carried out, but no data on this test is available.

Production tests

Both the Elmore No. 1 and the Sinclair No. 4 wells have been produced for extensive periods. In Fig.

39, the production-test data currently available for the Elmore No. 1 well is shown. No information is available for this test regarding this well's regulation, drawdown, the nature of the solids deposited, etc. A common method used to analyze rate data with regard to production is to plot the rate logarithmically as a function of cumulative flow. This plot can then be extrapolated to an abandonment condition, at which point the total reserve is noted. Such a plot of the production-rate data of Fig. 39 is shown in Fig. 40. We extrapolated the data as shown by the dashed line, ignoring the major excursions. If the data is fitted with a least-squares fit through all the data points, the depletion appears to be rapid. Since we do not have adequate information describing the test in which these data were measured, we are unable to draw convincing conclusions at this time with regard to reserves. The testing of the Sinclair No. 4 well has been recently terminated due to casing deterioration, and no data is available from that well either.

From the data shown in Fig. 36, the average flow rate from Magmamax No. 1 over a one-week period is about 50 kg/s. This is equivalent to 1450 $(kg/s)/m^2$. Both Magmamax No. 1 and Woolsey No. 1 were completed with 8-5/8-in. liners. Since the Woolsey well was completed in less productive strata, its flow rate should be less than the value given for Magmamax No. 1. From Fig. 35, we see the injection wells (Magmamax Nos. 2 and 3) were completed with 9-5/8-in. liners, but, as we have remarked earlier, reinjection will probably be limited by overpressure considerations rather than wellbore radius. Since the orifice value for test of the Elmore No. 1 well is not known, we cannot draw any conclusions about the absolute flow rate from the well test shown in Fig. 39. However, we can say that over the one-year test the flow rate did not diminish appreciably, although the well was periodically shut in.

SUMMARY OF FLOW CHARACTERISTICS

Drillstem tests (DST's) have been carried out during the drilling of the Magmamax No. 1 and Woolsey No. 1 wells. The DST's indicate permeabilities in the upper reservoir are very high--probably greater than 500 md. The porosity (and storage) of these strata are also quite large. However, the DST's also show that, in that part of the upper reservoir near the shale barrier separating the upper and lower reservoirs, the permeability is only about 250 md, and, in the lower reservoir (below the shale layer),

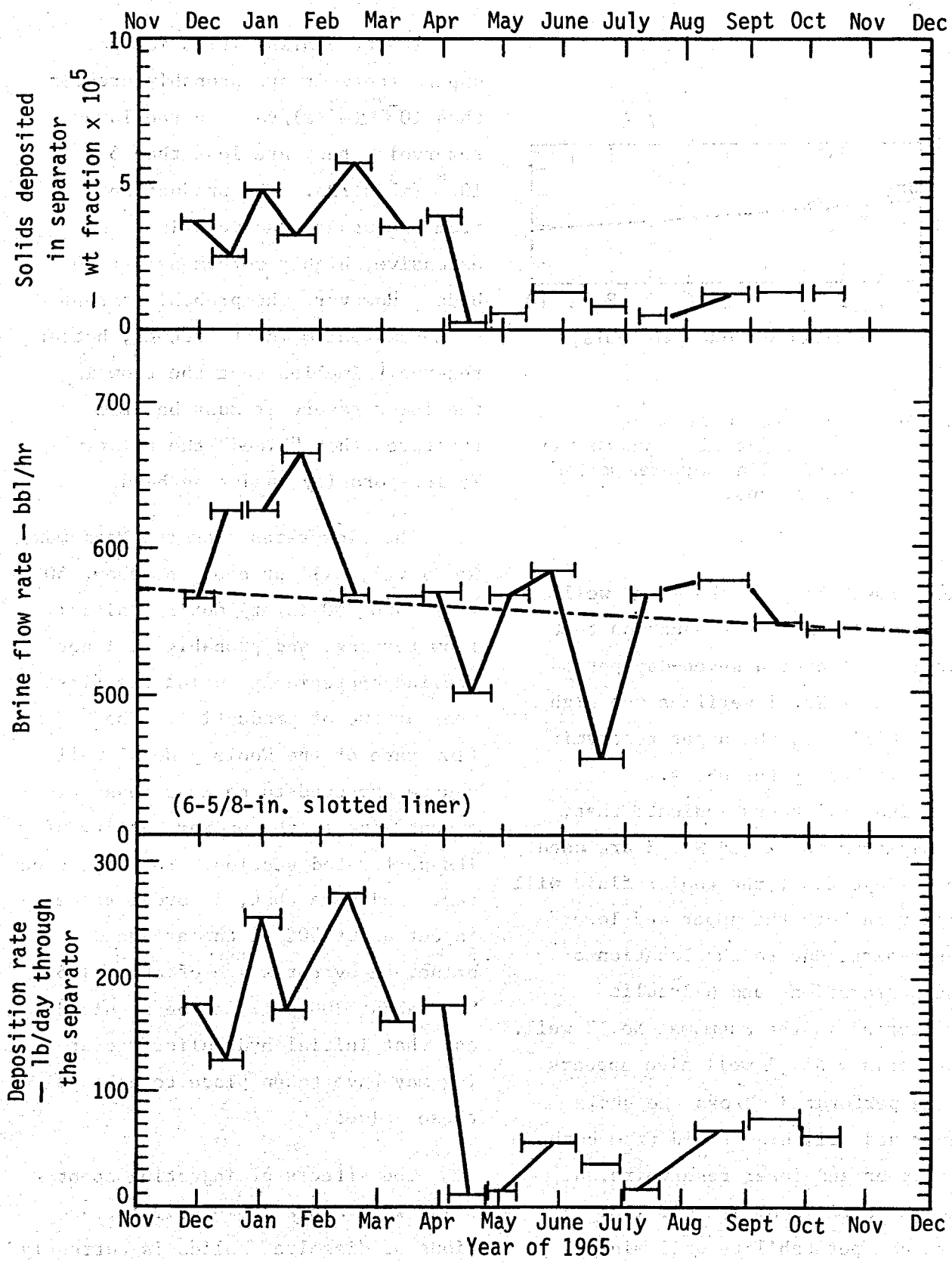

Fig. 39. The Elmore No. 1 Production Test showing flow rate and deposition.

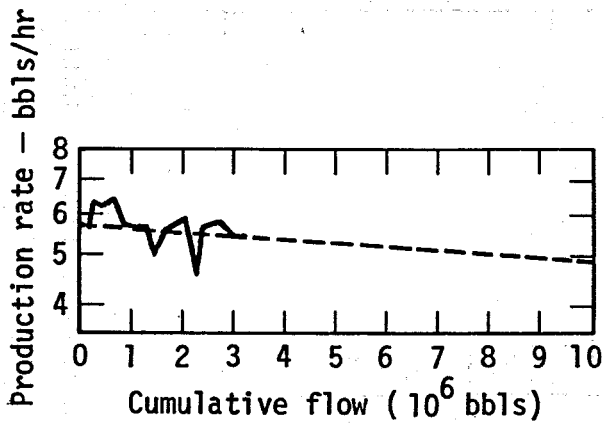

Fig. 40. The rate in terms of cumulative flow, where the dashed line ignores major excursions.

the permeability at these two wells is about 175 md. A production test carried out over a seven-day period at Magmamax No. 1 verifies the high permeability in the upper reservoir as indicated by the DST's.

The well tests indicate that, if Magmamax No. 2 and No. 3 are used for reinjection, the cooler fluid will appear in both the upper and lower reservoirs, due to the location of the perforations and hydraulic fracturing in the Magmamax No. 3 well. The Woolsey No. 1 well also appears to be perforated across the shale layer and will draw fluid from both the upper and lower reservoirs, although at the Woolsey well limited vertical permeability will minimize the contribution from the lower reservoir.

The transmissivities in the upper reservoir are probably greater than 10^{-7} $(m^3/s)/Pa$. In the lower reservoir, they are less than 5×10^{-8} $(m^3/s)/Pa$. The production from the upper reservoir is from extensive, highly porous sandstone beds. However, the probable extent of metamorphism in the deeper, hotter reservoir implies that the flow in the lower reservoir must be from fractures that "bleed" the relatively low-porosity sandstone beds.

The flow rates from the Magmamax No. 1 well will probably be about 50 kg/s (400 000 lb/hr) during initial flow testing, and probably will not decline appreciably during the first year or two of production. The flow rate of the Woolsey No. 1 well can be expected to be less than this amount, due to the poorer quality of its perforated section. The injection tests indicate that, in order to reinject about 50% of the produced brine, an overpressure of about 1.5 MPa (about 300 psi) may be required, and that initial hydraulic fracturing may have taken place to achieve these values.

The effects of injecting spent brine with appreciable weight fractions of dissolved solids is currently unknown. However, we note that at 50-kg/s flow rate, more than

4×10^6 kg of brine would be produced each day by each well. If half this brine is reinjected and the weight fraction of dissolved solids is assumed constant at about 1/4, then about 5×10^5 kg of dissolved solids will be injected into each well each day. Since the porosity in the lower reservoir is less than 20%, we might conclude that prolonged injection will be possible only if a) the injection wells are or will be in communication with a large aquifer (e.g., a large fracture, fissure, or fault), or b) the hotter reservoir rock heats the reinjected fluid sufficiently to redissolve any precipitates which may have formed prior to reinjection.

Field Production

The reservoir at the Magma-SDG&E site has not been produced over any extended period for which we have data, and detailed information for the extended well test of the Elmore No. 1 well is not available. Hence, our analysis of the reservoir is based on assumptions about how production will be carried out in the future. Clearly, this can lead to serious problems, and we stress the fact that this report is part of a preliminary study. Additional information may require modifications to our conclusions.

RESERVES

From the few extensive well tests we know of, we can estimate the proven reserves[33] of heat. Although not enough information is available to provide an extremely accurate estimate, we can make a first approximation based on what we presently know. We use the simple model of Matthews and Russell to compute reserve estimates from the well test data[26]. The estimated pore volume V_p perturbed during the well tests is given in m^3 by

$$V_p \approx \frac{\pi}{40} \left(\frac{t}{\beta}\right) \left(\frac{kh}{\mu}\right) \qquad (7)$$

where the symbols were defined in the analysis of DST's at Magmamax No. 1 in the previous section. The proven heat in the fluid (in GW•yr) is then given by*

$$E_f \approx \pi \rho \Delta H V_p \times 10^{-17} \qquad (8)$$

where ΔH is the enthalpy of the fluid referred to some standard temperature, which we take to be 25 C. The corresponding heat in the rocks is given by

*Here we have used the approximation 1 yr $\approx \pi \times 10^7$ s.

$$E_r \approx \frac{\rho_r(1-\phi)C_r}{\rho_f \phi C_f} E_f \qquad (9)$$

where C is the specific heat capacity, and the f and r subscripts refer to fluid and rock.

In Table 5 the calculated values of the proven reserves of fluid and heat from the wells with the most extensive well tests are shown.

When the reservoir fluid is produced and subsequently reinjected at a cooler temperature, the reinjected fluid quickly comes to thermal equilibrium with the porous reservoir rock. Hence, it is important to consider the heat energy stored in the rock and to include the heat in the rock in the reserve estimate. Since the Magma-SDG&E location is near large faults, we have also calculated the approximate radii of investigation for these tests, to see whether the fault could have been detected as a barrier during the well testing. In Table 6 these values are shown.

The radius at which a disturbance will be detected by these tests might be greater than the values of r_e in Table 6, because the actual lithology is a mixture of rocks with higher and lower permeability and porosity. In these estimates, the geology is assumed to be homogeneous, and this assumption effectively produces a mean value instead of the maximum value.

Table 5. Proven energy reserves for the fluid, E_f, from well tests (reservoir fluid in place — not electrical energy). The total compressibilities β are estimated values, while the transmissivities kh/μ are from well tests.

Well name	Length of test, days	β, Pa^{-1}	kh/μ, $(m^3/s)/Pa$	V_p, m^3	ΔH, J/kg*	E_f, GW·yr
Elmore No. 1	238	6×10^{-10}	5×10^{-8}	1.3×10^{8}	1.2×10^{6}	4.9
Magmamax No. 1	7	5×10^{-10}	1×10^{-7}	0.95×10^{7}	0.85×10^{6}	0.25
Sinclair No. 4	40	6×10^{-10}	5×10^{-8}	2.2×10^{7}	1.05×10^{6}	0.8
Totals				1.6×10^{8}		6

*From Ref. 17.

Table 6. Radius of investigation r_e and proven reserve of heat in the reservoir rock corresponding to the well tests.

Well	ϕ	ρ_r, kg/m^3	C_r, J/kg•K	C_f, J/kg•K	h,* m	r_e, m	E_r GW•yr
Elmore No. 1	0.16	2300	1090	4300	714	600	14.7
Magmamax No. 1	0.3	2200	1050	4200	142	266	0.32
Sinclair No. 4	0.16	2300	1090	4300	150	540	2.4
Total							17.4

*Length of perforated interval.

RESERVOIR DEPLETION

The reservoir fluid is believed to be at or near the saturation curve (for the appropriate salinity) at the Magma-SDG&E site. The reservoir will probably deplete similarly to oil reservoirs producing above the bubble point. This mode of production is known to deplete exponentially[34] and was the depletion mode at Wairakei during the early production period. If there are no influx or formation drives, the initial reservoir depletion can be quite rapid (depending on production level and resource size). Flashing in the reservoir is not expected to occur during the test period at the Magma-SDG&E site.

In the upper reservoir at the Magma-SDG&E site, the high porosity and permeability imply non-zero vertical permeability in the sandstone. In this formation, gravity segregation would probably occur, reducing the breakthrough time due to undercutting of the hot reservoir fluid by cooler reinjected fluid. In the lower reservoir, the permeability is low and there is a higher fraction of shale, hence the vertical mobility will probably be very small except for fracture effects, which at this time are undetermined.

If the production is from Magmamax No. 1 and Woolsey No. 1 (mainly upper reservoir wells), and reinjection is through Magmamax No. 2 and No. 3 (mainly lower reservoir wells), very little fluid will move from the injectors to the producers, because the major shale break separates the reservoirs. If the shale break does not completely separate the upper and lower reservoirs, some fluid may

migrate from the deeper Magmamax No. 2 and No. 3 wells to the shallower Magmamax No. 1 and Woolsey No. 1. At the present time this migration appears unlikely because the shale layer seems to effectively separate the upper and lower reservoirs. However, this apparent reservoir separation may also result in serious overpressure problems, making reinjection more difficult. The high porosity in the upper reservoir may also result in detectable subsidence, if appreciable fluid is withdrawn from the upper reservoir with only small amounts of fluid appearing from the injection wells.

The mobility ratio $(k/\mu)_{cold}/(k/\mu)_{hot}$ is believed to be favorable (less than unity), but if the vertical mobility is small and the upper and lower reservoirs are well separated, the stability of the injection front will not be a factor in well production. Similarly, breakthrough times — given the geology and well completions — depend heavily on which of the four Magma-SDG&E wells are flowed.

FLOW PATTERNS

We can summarize the <u>probable</u> flow patterns as follows.

- The Brawley fault is close enough to the four Magma wells (see Fig. 9) that, after a few weeks of production from the upper reservoir, the fault should appear as either a barrier or a conduit in the analysis of well tests.
- The upper reservoir rock appears to be of poorer quality at the Woolsey well than at the Magmamax wells. This may imply limited production from the southeastern portion of the upper reservoir.
- The flow in the lower reservoir will depend heavily on the fracture permeability, the extent of which is unknown at this time.
- The shale barrier dips to the northeast (see Fig. 10), and this suggests that between the "bounding" faults the flow pattern may dip also. There is no apparent reason to suspect any major <u>areal</u> anisotropy in flow patterns at the present time.
- The Woolsey and Magmamax No. 3 wells are not perforated in the most highly permeable sands and have part of the perforated interval lost to the large shale layer. The higher permeability and storage in the upper reservoir may result in preferred flow to or from the upper reservoir at these two wells.

EFFECTS OF FRACTURES

The presence of fractures does not necessarily imply a reduced well lifetime due to prefered flow from an injection well to a producing well. Kasameyer and Schroeder[35]

found that a reservoir with injection and production wells depletes as if the rock were completely porous, if the average spacing between distributed fractures is less than about 20 m. This sort of depletion results from the thermal diffusivity of the average reservoir rock (<20 m^2/yr), which allows sufficient heat to be removed from the rocks so that both rock and fluid are at about the same temperature. But widely spaced fractures — spaced more than 100 m — can drastically reduce the lifetime of production-injection well pairs when both wells intersect the same fracture and the fluid temperature decreases faster than the rock temperature.

SUMMARY OF FIELD PRODUCTION

We have not described in detail the extended well tests carried out at the Salton Sea because little information is available from them. However, what information is known from well drilling and testing has allowed us to estimate heat reserves within the upper reservoir as about 1/4 GW•yr in the fluid plus about 1/3 GW•yr in the rock. The heat reserves within the lower reservoir are about 5-3/4 GW•yr in the fluid plus about 17 GW•yr in the rock. The reserves implied from assumptions of lithological continuity are many times these numbers. Production from the upper reservoir might be accompanied by appreciable subsidence, if the entire reinjection is in the lower reservoir. If compaction does not occur, the well pressures might rapidly decrease, strongly affecting the well lifetimes.

The effects of possible fractures in the shale layer separating the upper and lower reservoir — in particular the effects on vertical mobility of the reinjected brine — must be determined to adequately characterize the reservoir's behavior during production and reinjection. The wells' completions will probably result in a large degree of separation during production and reinjection. The Brawley fault may affect extended production, because it is close to the Magma-SDG&E site. No information is currently available on the isotropy or anistropy of mobilities and flow patterns in the vicinity of the SDG&E experiment, although areal isotropy is assumed. The fracture spacing observed in wells in the SSGF imply that fractures will not degrade the thermal productivity at the Magma-SDG&E site, but the fracture spacing and well apertures at the Magma-SDG&E site are not well known and could play a role in thermal depletion of the reservoir.

Conclusions and Recommendations

CONCLUSIONS

The SDG&E experimental geothermal site is located in a tectonically active area, and is bounded by at least two active, northwest-trending faults which may influence the geothermal reservoir behavior during production and reinjection. The sedimentary deposit making up the reservoir rock is extensive and is saturated with brine throughout the high-temperature geothermal anomaly. The reservoir appears to be separated into an upper and lower portion by a shale layer. The upper reservoir is porous sand and shale with high permeability and productivity, bounded by a caprock at about 350 m and a shale barrier at about 800 m. The lower reservoir rock is sandstone, shale, and metamorphosed minerals and has much lower porosity and permeability. However, it has much greater thickness and is probably extensively fractured.

The temperatures in the upper reservoir range from 200 C at the caprock to almost 300 C at the shale barrier. In the lower reservoir, the temperatures may reach 360 C at depth. The total reservoir volume (fluid and rock), as defined by having a mean temperature above 200 C, probably exceeds 1.4×10^9 m^3. The weight fraction of dissolved solids in the fluid may be as high as 1/4, and this salinity and the associated acidity provide the most difficult, unsolved technological problems associated with extracting useful power from the reservoir.

The transmissivities obtained from well-test analyses are about 5×10^{-7} $(m^3/s)/Pa$ in the upper reservoir and 10^{-8} $(m^3/s)/Pa$ in the lower reservoir. The calculated proven reserves are about 1/4 GW•yr (in the fluid) and about 1/3 GW•yr (in the rock) for the upper reservoir, about 5-3/4 and 17 GW•yr (in the fluid and rock respectively) for the lower reservoir. Since the overall efficiency of extracting electrical power is probably about one-tenth (this includes plant efficiency, well-field sweep efficiency, etc.), the proven reserves of the upper reservoir appear capable of generating 10 MWe for at least five years. There is not enough evidence from well testing to predict depletion of the reservoir or to estimate abandonment conditions.

The injection tests indicate a possible problem in that the injection wells will have to be overpressured to achieve flow rates that

will accommodate the expected production of brine. In addition, an undetermined amount of the dissolved solids might appear in the form of a precipitate in the wellbore. Since a decrease by a factor of two in a rock's porosity can mean about three orders of magnitude decrease in its permeability,[36] it is imperative that these precipitates not reduce the pore space of the strata during reinjection.

RECOMMENDATIONS

The most serious limitation imposed on our well-test analyses is incomplete data. A complete reservoir characterization requires additional information from the well tests over a sustained period. Data are needed for both production and injection carried out in a prescribed manner in all available wells. To obtain the maximum amount of information, describing the locations of aquitards, aquifers, etc., sensitive downhole pressure gauges, which provide pressure-transient information, need to be developed to withstand the high temperatures in the wellbore. To allow computer simulation of the multiwell, production-injection phenomena, the downhole flowing temperatures and pressures are required at production, injection, and observation wells. These data are particularly important if hydraulic fracturing has already occurred.

Determining the extent of the geothermal resource requires additional geophysical measurements in the vicinity of the Magma-SDG&E site. The region under the current Salton Sea between the Brawley and Red Hill Faults is of special interest and should be explored by drilling as soon as possible. Slant-hole methods could provide information relatively quickly about this portion of the Salton Sea KGRA, without requiring special drilling platforms.

The nature of the precipitates that will appear at the reinjection well after the brine has been cooled is a critical question. Chemistry experiments to be conducted by Lawrence Livermore Laboratory personnel in cooperation with SDG&E may provide some answers to this latter, exceedingly important question.

Acknowledgments

This report would not have been possible without the coordinated efforts of the people in the LLL Geothermal Geology Group. They are: J. H. Howard, P. W. Kasameyer, C. R. McKee, L. B. Owen, T. D. Palmer, J. D. Tewhey, and D. F. Towse.

Notes and References

1. T. C. Hinrichs, "San Diego Gas and Electric Company—Magma Power Company Wells," in *Geothermal Development of the Salton Trough, California and Mexico*, T. D. Palmer, J. H. Howard, and D. P. Lande, Eds., Lawrence Livermore Laboratory, Rept. UCRL-51775 (1975), p. 30.
2. H. W. Menard, *Science* 132 (3441), 1737 (1960).
3. D. P. Hill, P. Mowinckel, L. G. Peake, *Science* 188 (4195), 1306 (1975).
4. V. C. Kelley and J. L. Soske, *J. Geol.* 44, 496 (1936).
5. P. T. Robinson, W. A. Elders, and L. J. P. Muffler, *Geol. Soc. Amer. Bull.* 87, 347 (1976).
6. S. Meidav, and R. Furgerson, *Geothermics* 1, 47 (1972).
7. D. Towse, *An Estimate of the Geothermal Energy Resource in the Salton Trough, California,* Lawrence Livermore Laboratory, Rept. UCRL-51851, Rev. 1 (1976).
8. S. Biehler and P. Kasameyer, Lawrence Livermore Laboratory, private communication (June, 1976).
9. T. Lee, University of California, Riverside, private communication (June, 1976).
10. *The Colorado River and Imperial Valley Soils,* Imperial Irrigation District, Bulletin 373 (1973).
11. L. A. Tarbet, *Bull. Amer. Assoc. Pet. Geol.* 35 (2), 260 (1951).
12. O. J. Loeltz, B. Irelan, J. H. Robinson, and F. H. Olmsted, *Geohydrologic Reconnaissance of the Imperial Valley, California,* United States Geological Survey, Paper 486-K (1975).
13. L. J. P. Muffler and B. R. Doe, *J. Sed. Pet.* 38 (2), 384 (1968).
14. D. Towse and T. D. Palmer, *Summary of Geology at the ERDA Magma-SDG&E Geothermal Test Site,* Lawrence Livermore Laboratory, Rept. UCID-17008 (1976).
15. L. C. Dutcher, W. F. Hardt, and W. R. Moyle, Jr., *Preliminary Appraisal of Ground Water Storage with Reference to Geothermal Resources in the Imperial Valley Area, California,* United States Geological Survey, Circular 649 (1972).
16. L. J. P. Muffler and D. E. White, *Active Metamorphism of Upper Cenozoic Sediments in the Salton Sea Geothermal Field and the Salton Trough, Southeastern California,* Geologic Society of America, Bulletin 80 (1969).
17. H. C. Helgeson, *Amer. Jorn. Sci.* 266, 129 (1968).

18. P. Kasameyer, Lawrence Livermore Laboratory, private communication (Sept. 1975).
19. Schlumberger Co., private communication (November, 1972).
20. T. D. Palmer, *Characteristics of Geothermal Wells Located in the Salton Sea Geothermal Field, Imperial County, California,* Lawrence Livermore Laboratory, Rept. UCRL-51976 (1975).
21. T. D. Palmer, *Salton Sea Geothermal Field, Energy Assessment, Magma Power Company Property,* Lawrence Livermore Laboratory, Geothermal Geology Group, Internal Mem. GG-1 (1976).
22. S. Biehler, "Gravity Studies in the Imperial Valley," in *Cooperative Geological-Geophysical-Geochemical Investigations of Geothermal Resources in the Imperial Valley Area of California* (University of California, Riverside, 1971), P. 29.
23. L. B. Owen, Lawrence Livermore Laboratory, private communication (May, 1976).
24. L. B. Owen, *Precipitation of Amorphous Silica from High-Temperature Hypersaline Geothermal Brines,* Lawrence Livermore Laboratory, Rept. UCRL-51866 (1975).
25. H. J. Ramey, Jr., Lawrence Livermore Laboratory, private communication (December, 1975).
26. C. S. Matthews and D. G. Russell, *Pressure Buildup and Flow Tests in Wells, Monograph Volume 1, H. L. Doherty Series* (Society of Petroleum Engineers, Dallas, Tex., 1967).
27. H. N. Hall, *Pet. Tran. AIME* 198, 309 (1953).
28. J. H. Keenan, F. G. Keyes, P. G, Hill, and J. G. Moore, *Steam Tables* (John Wiley and Sons, New York, 1969).
29. W. H. Somerton, *Pet. Trans, AIME* 213, 377 (1958).
30. W. H. Somerton, *Pet. Trans. AIME* 219, 437 (1960).
31. W. C. Murphy, *The Interpretation and Calculation of Formation Characteristics from Formation Test Data* (Haliburton Services, Duncan, Okla.).
32. T. K. Perkins and L. R. Kern, *J. Pet. Tech.* 13, 937 (1961).
33. "Proven reserves" as used in this report should not be confused with phrases of others used to describe estimated amounts of geothermal energy. "Proven reserves" here refers to the sum of: 1) the product of the volume of fluid *perturbed by the well tests* discussed in this report and an average energy content per unit volume of fluid (note Eqs. 7 and 8) and 2) the

product of the volume of rock containing this fluid and the average energy content per unit volume of rock. Estimates of proven reserves apply only to a part of the Salton Sea Geothermal Field. Estimates of "indicated resource" and "inferred resource", etc., for the entire field and KGRA are discussed in Ref. 7. The "proven reserves" discussed in this report are a part of the total "indicated resource".

34. F. Brons, "On the Use and Misuse of Production Decline Curves," paper No. 801-39E, presented at the Spring Meeting of the Pacific Coast District, Division of Production, American Petroleum Institute (Los Angeles, 1963).

35. P. W. Kasameyer and R. C. Schroeder, "Thermal Depletion of Liquid Dominated Geothermal Reservoirs with Fracture and Pore Permeability," in *Geothermal Reservoir Engineering* (Stanford University, Stanford, California, 1975), SGP-TR-12.

36. M. Muskat, *Physical Principals of Oil Production* (McGraw-Hill, New York, 1949), P. 172.

FW/gw/vt/gw